

# RSC Applied Polymers

Accepted Manuscript

This article can be cited before page numbers have been issued, to do this please use: A. K. Yadav, N. Mohammad, E. Chamanehpour, Y. K. Mishra and P. K. Khanna, *RSC Appl. Polym.*, 2024, DOI: 10.1039/D4LP00093E.



This is an Accepted Manuscript, which has been through the Royal Society of Chemistry peer review process and has been accepted for publication.

Accepted Manuscripts are published online shortly after acceptance, before technical editing, formatting and proof reading. Using this free service, authors can make their results available to the community, in citable form, before we publish the edited article. We will replace this Accepted Manuscript with the edited and formatted Advance Article as soon as it is available.

You can find more information about Accepted Manuscripts in the [Information for Authors](#).

Please note that technical editing may introduce minor changes to the text and/or graphics, which may alter content. The journal's standard [Terms & Conditions](#) and the [Ethical guidelines](#) still apply. In no event shall the Royal Society of Chemistry be held responsible for any errors or omissions in this Accepted Manuscript or any consequences arising from the use of any information it contains.

## Data Availability Statement

### **Polyaniline (PANI) Nano-Composites with Se, Te and their metal chalcogenides: A Review**

Alok Kumar Yadav<sup>a</sup>, Naeem Mohammad<sup>a</sup>, Elham Chamanehpour<sup>b</sup>, Yogendra Kumar Mishra<sup>b</sup>, and Pawan K. Khanna<sup>\*a</sup>

Being the review article various data presented in the manuscript are from the literature and they are presented in the manuscript with permission. The copyright permission obtained is available with authors and will be provided on demand.

The original data if required may be demanded from the original author of the referred articles.



## REVIEW

**Polyaniline (PANI) Nano-Composites with Se, Te and their metal chalcogenides: A Review**Alok Kumar Yadav<sup>a</sup>, Naeem Mohammad<sup>a</sup>, Elham Chamanepour<sup>b</sup>, Yogendra Kumar Mishra<sup>b</sup>, and Pawan K. Khanna<sup>\*a</sup>Received 00th January 20xx,  
Accepted 00th January 20xx

DOI: 10.1039/x0xx00000x

Research over the past four decades has matured polyaniline and most preferred conducting polymers and several methods have been proposed by researchers for its synthesis and conversion to various forms of polyaniline (PANI) as well as its doping with chalcogens specially selenium (Se) and tellurium (Te) have been explored using various chemical methods and their different properties are extensively studied in terms of electrical, thermal, morphological and optical behaviour. This review summarizes, the results from research experiments, including their synthesis and characterization as well as study of various properties viz; DC conductivity measurements, scanning electron microscopy (SEM), Fourier Transform Infrared Spectrometry (FTIR), field emission studies, EMI shielding behaviour, electrochemical, supercapacitive, optoelectronic and thermoelectric properties. The incorporation of chalcogens into PANI leads to a significant improvement in electrical conductivity and field emission properties, making these nanocomposites promising materials for various electronic applications. The global energy crisis underscore the need for innovative materials for energy solutions. Solution-based polymer thermoelectric (TE) technologies offer an eco-friendly and cost-effective approach to convert heat into electricity. Successful electrodeposition of tellurium films onto phenolic foam with PANI coatings and the synthesis of a novel PANI/Te nanocomposite with enhanced nonlinear optical properties open up new avenues. These nano-composites were prepared using different methods, including simultaneous electrochemical reactions, *in-situ* polymerization, and interfacial polymerization.

**1. Introduction**

Advanced materials such metals and ceramics including polymer composites are versatile materials and are the basis for modern technological advancement. The advent of conducting polymers (CP) was a significant finding by the researchers where they demonstrated that the conductivity can be increased by adding electron acceptors in polyacetylene which won the year 2000 Nobel prize to Shirakawa, Heeger, and MacDiarmid.<sup>1-2</sup> One of the well-known and extensively researched conducting polymers is Polyaniline (PANI). PANI has been doped with a range of chemicals, including protonic acids and oxidants, and can be tailored to ease of processing into various forms, such as coatings. PANI has been useful for range of applications, including batteries<sup>3</sup> supercapacitors<sup>4</sup> and sensors.<sup>5</sup> It is environmentally sustainable and stable, relatively inexpensive, and simple to synthesize, and has a high charge storage density. The oxidation and protonation states of polyaniline govern its physical and electrochemical properties.<sup>6</sup> PANI has been

considered a desirable conductive material since its discovery to synthesize conductive composites for a variety of uses, including electro-magnetic (EM) absorption particularly microwave absorption, dissipation of electricity, heating probes, conducting glues, conducting membranes, anticorrosion paint/coatings, and sensor materials.<sup>5,7-9</sup> Despite PANI has a variety of uses in large-scale industrial applications, many of its prospective uses have not yet been fully investigated due to limitation in its processing. The best preparation strategies and very accurate molecular design are therefore desired to be practiced to synthesize primary conducting polymers. Typically, polymerization of aniline leads to formation of polyaniline which has conjugating structure with rigid backbone i.e. alternate single-double bond. Researchers have proposed that PANI can exist in several oxidation states<sup>8,10</sup>

1. Leucoemeraldine- a fully reduced form of polyaniline
2. Pernigraniline- said to be a fully oxidized form of polyaniline
3. Emeraldine Salt/Base-a green/blue as oxidized: reduced (1:1)

Amongst them, the Emeraldine is the most conductive form of PANI. The conductivity of Emeraldine Base (EB) is lower than that of Salt (ES) because EB exhibits semiconducting nature while ES has metallic conductivity. When the emeraldine base undergoes protonation to become the emeraldine salt, a structural transformation occurs due to the mechanism of proton-induced spin unpairing. Consequently, this leads to a band that is half-filled, and it may potentially give rise to a metallic state where each repeat unit carries a positive charge due to protonation, along with an associated

<sup>a</sup> Quantum Dots/Nanomaterials Laboratory, Department of Applied Chemistry, Defence Institute of Advanced Technology, Pune 411025, India

<sup>b</sup> University of Southern Denmark, Alsion 2, 6400, Sønderborg, Denmark

\* Corresponding Author E-mail: pawankhanna2002@yahoo.co.in, khannap@diat.ac.in

Electronic Supplementary Information (ESI) available: [details of any supplementary information available should be included here]. See DOI: 10.1039/x0xx00000x



counter ion. Conductivity is also affected by the synthesis processes and the parameters involved. Conductivity of EB has been reported to increase with acid doping.<sup>8</sup> Aqueous solutions of acids such as camphor sulfonic acid (CSA), picric acid, phosphoric acid, sulfuric acid, and hydrochloric acid were used for doping EB PANI. With limitation in its dissolution behaviour, practical applications become difficult. The difficulty in processibility is because of possible hydrogen bonding between atoms of adjacent chains and a stiff polymer backbone. The melt processing of PANI is also excluded because of instability of EB form at melt processing temperatures.<sup>8,10</sup> Due to its distinctive oxidation states, the doping mechanism in polyaniline stands out among all conducting polymers. In the light of the aforementioned discoveries, the core idea of polyaniline synthesis, doping, and conduction mechanism offers in-depth research for both additional technological applications and fundamental scientific interest.<sup>8-11</sup> Several metals have been incorporated in polyaniline to study its properties, which includes Ag/PANI<sup>12</sup>, Au/PANI<sup>13</sup>, Zn/PANI<sup>3</sup>, Pt/PANI<sup>14</sup> etc. Sezer *et al.*<sup>12</sup> have measured intensity dependent refractive index and found PANI/Ag nanocomposite suitable for optical pulse compression and limiting due to its reversible absorption behaviour at same wavelength. Li *et al.*<sup>13</sup>, constructed AuNPs@PANI nanospheres by oxidizing aniline by HAuCl<sub>4</sub> oxidant with simultaneous formation of Au NPs. Zhihua *et al.*<sup>3</sup> have incorporated Zn microspheres into self-assembled hollow microspheres of PANI to make PANI hollow microsphere/ Zinc composite. Zhang *et al.*<sup>14</sup>, have deposited PANI array on carbon cloth by chronoamperometry (applying a time dependent square wave potential to working electrode), then on Pt nanosheet by amperometry (applying constant potential to working electrode) to detect ammonia. Likewise, several metal oxides have also been introduced into polyaniline network to generate variety of conducting polymer nano-composites. This includes ZnO/PANI<sup>15</sup>, CdO/PANI<sup>16</sup>, CuO/PANI<sup>17</sup>, TiO<sub>2</sub>/PANI<sup>18</sup>, etc. Gheymasi *et al.*<sup>15</sup>, had copolymerized aniline and pyrrole using ammonium peroxydisulphate (APS) as an oxidant and T-X100 as an emulsifier, then blended it with ZnO nanoparticles in CHCl<sub>3</sub> solution and obtained self-focusing and reverse saturation absorption which can lead to its use in protection of eyes and optical instruments from lasers of high intensity. Roy *et al.*<sup>16</sup> reported

CdO/PANI composite via an in-situ polymerization process using aniline-HCl-CdO solution and APS. Due to structural changes by introduction of CdO, conductivity had increased. In small frequency region, AC conductivity had shown deviation from Jonscher power law based on dipole polarization effect,  $\sigma(\omega) = \sigma_0 + A \omega^n$ . Thampi *et al.*<sup>17</sup> had grown brown coloured 50 nm NPs of CuO using Copper Nitrate and Polyethylene glycol and immobilized them in PANI matrix by *in-situ* polymerization of aniline. So-generated composite was incorporated in woven and non-woven cotton fabric by immersing it in PANI/CuO solution for anti-bacterial purpose. Gapusan *et al.*<sup>18</sup> have immobilized TiO<sub>2</sub> NPs into PANI-coated kapok fibre by hydrothermal method. They demonstrated photocatalytic activity against Methyl Orange (MO) and Cr (IV) and antibacterial property against E. coli under visible light. Similarly, a variety of other oxide nanoparticles, such as TiO<sub>2</sub>, CeO<sub>2</sub>, ZrO<sub>2</sub>, Fe<sub>2</sub>O<sub>3</sub>, Fe<sub>3</sub>O<sub>4</sub>, ZnO, and CdO can be incorporated into polymer matrix and are useful for a variety of applications in various scientific and technological fields.<sup>10, 16-18</sup>

## 2. PANI-chalcogen (Se & Te) Nanocomposite:

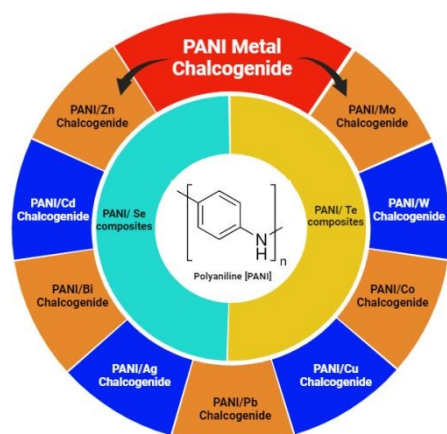
Chalcogens are the element of group 16 (O, S, Se, Te and Po). However, oxygen and polonium are not considered as true chalcogens. Oxygen (O<sub>2</sub>), mainly due to its difference in chemical properties owing to the un-availability of vacant d-orbitals however, while in heavier chalcogens vacant d-orbitals are present so they show diverse chemical and physical properties. The electronegativity (EN) of oxygen is much higher than those of the other chalcogens. Polonium is a heavier element as well as radioactive element. The chemical properties of selenium and tellurium opened up new avenues in the field of electrical and opto-electronic applications therefore, inorganic metal chalcogenides attracted immense attention of researchers globally. In recent times, the Se and Te based nanocomposite made huge impact due to their superior electrical, thermal and optical properties. This has also extended to their nano-composites with conducting polymers e.g. PANI for further advancement. Amongst the conducting polymers, polyaniline has not been widely studied with Se and Te. Combination of them as a nanocomposite can bring significant changes in their properties. Thus, the scope of this review is limited to investigating the effects of incorporation selenium (Se), tellurium (Te) and their inorganic selenides and tellurides on the properties of PANI. Some research has been conducted on these materials to discover applications in supercapacitors, thermoelectric, electrical, opto-electronic, medicinal and other fields (Table 1).

### 2.1 Polyaniline/Selenium (PANI/Se) Nanocomposites:

Chemical methods have been largely investigated for the synthesis of Se/PANI nanocomposite mostly by following two main approaches for doping of Se in polyaniline<sup>11, 19-21</sup>

- By mixing Se before polymerization in aniline solution
- By doping Se in PANI EB solution after polymerization

Each method significantly impacts the structural, electrical, and morphological properties of the resulting nanocomposite, making the choice of synthesis technique crucial. For instance, it has been demonstrated that PANI can be synthesized through chemical oxidation of aniline using APS and its composite with Se on Si-substrate can be studied to understand the nature of film in terms of



**Scheme 1.** Bird's eye view of various PANI/chalcogen composites



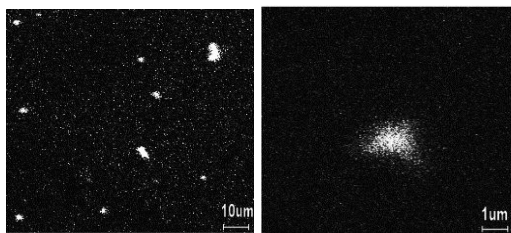


**Figure 1.** TOF-SIMS image of Se distribution in PANI film [Reproduced from ref. 19, with permission from Elsevier, copyright 2003]

the distribution of Se in the PANI matrix, using time-of-flight secondary ion mass spectroscopy (TOF-SIMS).<sup>19</sup> This has revealed a uniform distribution of selenium with both submicron dots and clusters where larger clusters have higher concentration of Se than average Se concentration (Fig.1). Such distribution patterns are crucial as they influence the composite's electronic and optical properties. Similarly, Shumaila *et al.*<sup>20</sup> demonstrated that Se nanowire (45-75 nm diameter) prepared using SeO<sub>2</sub>, β-cyclodextrin and Vitamin-C, can be mixed with PANI EB ultrasonically in chloroform to form PANI/Se nanocomposite. This composite exhibit potential in vacuum microelectronic devices and plastic display industries for field emission behaviour. On the application of high electric field electrons can be emitted by quantum tunnelling. This emission is dependent on the work function of the material and its field enhancement factor.<sup>20(a)</sup> Utilizing an *in-situ* approach, Ozkazanc *et al.*<sup>21</sup> prepared PANI/Se composite by mixing pre-dissolved selenium in nitric acid with aniline and APS, followed by spin coating. Their work highlighted a distinct FTIR peak associated with Se-Se stretching vibrations at 872 cm<sup>-1</sup>, indicating successful incorporation of selenium into the polymer matrix. This method has shown that varying the concentration of selenium can modulate the band gap and conductivity of the composite, which are vital for optimizing the material for specific electronic applications such as transistors and diodes. Band gap can be engineered by the doping of Se in PANI, via doping process and can be evaluated by optical measurement and such a doping can increase conductivity to three orders of magnitude<sup>11</sup>. The initial morphology of selenium nano-particles itself may influence morphology of PANI/Se nano-composite if the composite is generated via an ex-situ processing however via an in-situ processing morphology can be controlled by reaction parameters and the reagents employed to generate selenium.

Over all spherical Se particles doping leads to granular cluster structures while with doping with Se nanowire, a fibrous interwoven morphology was observed by the researchers where it was believed that such an arrangement may provide effective conductive pathway due to movement of delocalized electrons along conjugated pathways and electron hopping mechanism between the adjacent redox sites within polymer chain. FTIR spectra show structural changes in PANI after Se doping and provide evidence for interaction of Se with the polymer chain. It has been opined that due to electrostatic interaction between nitrogen atoms and selenium ion physical adsorption of Se on PANI molecule is also possible.<sup>21</sup>

Researchers have also investigated field emission behaviour of PANI/Se nanocomposites using indigenously fabricated setup at room temperature maintaining a pressure of 10<sup>-6</sup> Torr in a vacuum chamber demonstrating that 10% (w/w) Se doping showed the highest emission characteristics with low turn-on field of 1.2 V/m, making it promising material for field emission-based applications.<sup>20</sup> Moreover, novel composites like Graphene/Se/PANI have been reported to show superior performance in Li-ion battery application,

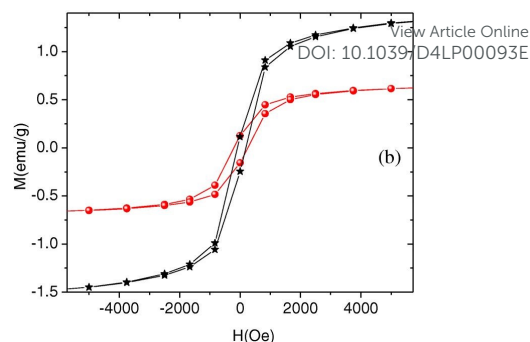


**Figure 2.** Room temperature magnetization curves for PANI/Se<sub>0.95</sub>Fe<sub>0.05</sub> (5 wt% in black and 10 wt% in red) nanocomposites [Reproduced from ref. 24, with permission from Springer, copyright 2019]

and displayed improved cycling durability and excellent performance at high rates, demonstrating a reversible discharge capacity (after 200 cycles) of 567.1 mAhg<sup>-1</sup> at 0.2 C and 510.9 mA h/g at 2C.<sup>22</sup> The nanocomposite robust electrochemical performance demonstrated its potential as cathode material for Li-Se batteries. Another innovative approach by Ye *et al.*<sup>23</sup> involved creating UIO-67@Se/PANI composites for Li-Se batteries using Zr-based metal-organic frameworks (MOFs) coated with PANI. This composite demonstrated significant specific capacities and retention rates, highlighting the versatility of Se/PANI composites in energy storage applications. Specifically, it achieved a notable specific capacity of 248.3 mAhg<sup>-1</sup> at 1C after 100 cycles, while maintaining capacity of 203.1 and 167.6 mAhg<sup>-1</sup> at higher rates of 2C and 5C, respectively. Heiba *et al.*<sup>24</sup> conducted a synthesis of polyaniline (PANI) combined with Se<sub>0.95</sub>Fe<sub>0.05</sub> at different weight ratios (5% and 10%) using an *in-situ* polymerization technique. Analysis using XRD verified the structural properties of PANI and the presence of Se<sub>0.95</sub>Fe<sub>0.05</sub>. It indicated a semi-crystalline structure for PANI and the emergence of Se<sub>0.95</sub>Fe<sub>0.05</sub> in two phases (trigonal-Se and orthorhombic-FeSe<sub>2</sub>) within the PANI nanocomposites (Fig. 2). The nanocomposites exhibited weak ferromagnetic behaviour, with enhanced coercivity and saturation of magnetization as weight percentage of Se<sub>0.95</sub>Fe<sub>0.05</sub> in PANI increased. The synthesis and characterization of selenium/polyaniline (Se/PANI) nanocomposites offer exciting insights for its diverse applications. Se doping in PANI has achieved through methods such as chemical oxidation and *in-situ* polymerization, influencing electrical, morphological, thermal, structural and optical properties. These nanocomposites show promise in fields like electronic devices, field emission applications, and energy storage systems. Future research avenues could focus on fine-tuning synthesis approaches, understanding the fundamental interactions between Se and PANI, exploring their performance in practical devices, and optimizing their properties for enhanced functionality and sustainability. Additionally, investigating novel composite architectures and exploring their applications in emerging technologies like Li-ion batteries and environmental remediation could further expand scope of Se/PANI nanocomposites. It is possible to propose that Se/PANI nano-composite might act as precursor of Se for metal selenide QDs/PANI nanocomposites.

**2.2 Polyaniline/Tellurium (PANI/Te) Nanocomposites:** The global energy crisis necessitates innovative energy solutions, which often depend on use of technologically much advanced polymer-composites materials as they are highly suitable for a range of energy



**Table 1.** Polyaniline/Chalcogen nanocomposites

Material	Synthesis Process	Significant Properties	Ref.
Se/PANI	Chemically doped by dissolving Se in Chloroform in EB form of PANI.	Electronic: DC conductivity	11
Se/PANI	Se pellets added in PANI EB solution in DMSO and heated	Optoelectronic	19
Se NW/PANI	Se nanowire is doped in swollen EB PANI by dissolving in Chloroform.	Field emission	20
Se/PANI	Polymerized after mixing Se and Aniline solution.	Electronic: AC conductivity	21
G-Se/PANI	GO added during polymerization of aniline on Se nanowire	Electrochemical: discharge capacity	22
UIO-67@Se/PANI	Aniline polymerized on UIO-67@Se powder	Electrochemical: Specific capacity	23
Se <sub>0.95</sub> Fe <sub>0.05</sub> / PANI	In situ polymerization	Optoelectronic: CIE coordinates, magnetization	24
Te/PANI/microporous phenolic foam	Galvanostatic deposition of Te on PANI coated phenolic foam.	Thermoelectric (TE)	25
Te/PANI	PANI EB doped with acidic solution of Te.	Electronic: DC conductivity	26
Te/PANI	Te catalyzed polymerization of aniline using Hydrazine Hydrate forming polyaniline coated Te nanowire.	Nonlinear Optical (NLO) property	27
PANI/Te Nanorod	Te nanorod dispersion in m-cresol used for doping in CSA-doped EB PANI.	Thermoelectric (TE)	28
PANI/Se-Te on LLC template	After potentiostatic polymerization of Aniline Brij56 LLC template, mesoporous Se-Te layer was electrodeposited using Se-Te Brij56 LLC electrolyte.	Electrochemical	29
PANI/SWNT/Te	Aniline in-situ polymerized with SWNT & Te attached hydrothermally later	Thermoelectric	30
(MWCNTs)-Te nanorod/ PANI	Te & MWCNT dispersed in m-cresol ultrasonically and mixed with PANI – m-cresol solution	Thermoelectric, transport parameters	31
PANI/Te	Following 28	Thermoelectric	32
Te <sub>x</sub> S <sub>y</sub> / Polyaniline	Single step nonlinear electrochemical	Electrochemical Impedance	33
Te/PANI	Te incorporated in PANI solution	Electrochemical, charge-transport mechanism	34
Te/PANI	In situ polymerization of aniline with tellurium	EMI shielding	36

applications including thermoelectric (TE) technologies offering an environmentally friendly and cost-effective means to convert low-grade heat into electricity. This section explores the synthesis and characterization of PANI/Te hybrid films and study of their thermal, electrical and optical properties. There are several methods adopted by the researchers for the preparation of PANI/Te nanocomposites. One of the methods discusses electrodeposition of Te film above PANI-coated phenolic foam. While the other method described use of acidic aq. solution of Te and its reaction with PANI for fabrication of PANI/Te nano-composite. It was reported that Te film can be electrodeposited onto phenolic foam using PANI coatings as conducting transition layers.<sup>25</sup> The structural and thermoelectric behaviour of the deposited films exhibited uniformity and preferred crystal orientation along the c-axis direction.

Thermopower measurements revealed maximum value of 342  $\mu\text{V}/\text{K}$  at 473 K, showcasing their thermoelectric potential. Kazim *et al*<sup>26</sup> reported doping of PANI with varied Te concentration in order to improve electrical properties of the composite. The maximum dc conductivity was found to be  $6.635 \times 10^{-5} \Omega^{-1} \text{cm}^{-1}$  for 25% Te doping. It was discussed that  $\text{Te}^{2+}$  doping results in carrier delocalization, due to attraction between neighbouring polymeric units arising out of incorporation of Te into the PANI chain. Such arrangement led to polaron and bi-polaron formation thus enhancing the carrier mobility with increased doping level of  $\text{Te}^{2+}$ . Also discussed about variation in doping concentration for achieving useful properties.

It was proposed that the electron delocalization in the composite occurs due to the presence of dopant and sulfuric acid together and they perhaps act as double doping reagents.<sup>26</sup> In another synthesis process, freshly prepared Te from  $\text{H}_2\text{TeO}_3$  via hydrazine hydrate, was used as catalyst in polymerization of aniline to prepare PANI coated Te nanowire, a broom-shaped hierarchical structure demonstrated superior NLO behaviour in comparison to individual components as per the authors discussion.<sup>27</sup> Wang *et al.*<sup>28</sup> employed ultrasonic dispersion method to form Te/PANI film that exhibited enhanced thermoelectric figure of merit (zT). The film showed  $146 \mu\text{W}/\text{mK}^2$  power factor and zT was enhanced from 0.156 at room temperature to 0.223 at 390 K. Nanocomposite with chalcogen alloy i.e., PANI/Se-Te nanocomposite has been synthesized and studied<sup>29</sup> by electrodeposition on a Brij56 (surfactant) Lyotropic Liquid Crystalline (LLC) template.

The integration of polyaniline (PANI) with tellurium (Te) in nanocomposites presents a promising avenue for enhancing thermoelectric (TE) application. It is mentioned that the synthesis and characterization of PANI/Te hybrid films exhibited improved thermoelectric properties, owing to well-matched nanoscale interfaces, enhanced carrier transport, and low thermal conductivity. Wang *et al.*<sup>30</sup> had followed innovative approach for in-situ synthesis of water-soluble ternary PANI/SWNT/Te (polyaniline/ single walled nanotube/ tellurium) nanocomposites, showing uniform structures and remarkable thermoelectric (TE) properties. The nanocomposite films demonstrated exceptionally high Seebeck coefficient accredited to energy filtering action at PANI/SWNTs along with PANI/Te interfaces, maintaining good balance between electrical thermal conductivity ( $0.2$  to  $0.4 \text{ Wm}^{-1}\text{K}^{-1}$ ) with TE power factor reached  $101 \mu\text{Wm}^{-1}\text{K}^{-2}$ , surpassing individual components present in the composite (Figure 3). The presented approach opens possibilities for designing high-performance ternary organic-inorganic composite TE materials with various fillers.

In another study an interfacial engineering was employed<sup>31</sup> which intelligently crafted Te based ternary hybrid nanomaterials tellurium nanorods, MWCNTs and PANI. Interactions among MWCNTs and Te nanorods, with PANI lead to well-bonded interfaces, enhancing electrical conductivity and thermopower simultaneously. The optimized composition resulted in a power factor of  $54.4 \mu\text{Wm}^{-1}\text{K}^{-2}$  (Figure 4). This research offered technically improved approach for enhancing the thermoelectric performance of conducting polymer-based hybrids, suggesting promise for economical flexible energy conversion devices suitable for large-scale production.

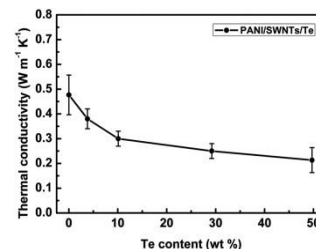


**Figure 3.** Thermal conductivity variation with Te content in the PANI/SWNT/Te nanocomposite [Reproduced from ref. 30, with permission from Royal Society of Chemistry, copyright 2017]



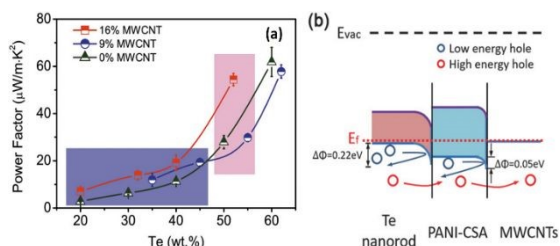


**Figure 4.** (a) TE properties comparison, (b) Interfacial energy filtering effects [Reproduced from ref. 31, with permission from Wiley VCH, copyright 2018]

Furtherance of this field was continued by Wang *et al.*<sup>32</sup> where they directed their attention towards enhancing the carrier concentration by subjecting polyaniline/Te nanorod hybrid films to thermal treatment. The outcome demonstrated that thermal treatment effectively tuned the carrier concentration, leading to a notable enhancement in thermoelectric electric performance. The study revealed that the hybrid film produced at 180°C exhibited a 20% increase in power factor compared to the original film by controlling dopant quantity and carrier concentration via thermal processing. Cathode material for Li-ion battery with high conductivity and capacity was discussed by Li *et al.*<sup>33</sup> showing potential of tellurium in this field. Such Te containing PANI composites exhibited large initial capacity and maintain cycling stability at 5 Ag<sup>-1</sup>, suggesting sustainable strategy for battery fabrication. The approach and designed nanorod structure presented promising solution for challenges associated with tellurium-based batteries. Rani *et al.*<sup>34</sup> fabricated a Te/PANI nanocomposite by solid-state chemistry method with vary in Te concentrations (5%, 10%, and 15%) that was blended with PANI. The resulting composite displayed adaptability for various energy harvesting purposes, including both conversion and storage. The successful integration of Te into the matrix at benzenoidal functionality, with oxygen bonding via sulphonated disorder, contributed to its super-capacitive behaviour. The authors concluded 10% Te concentration could be optimal for achieving both photo and electrochemical conduction performance.<sup>35</sup> Recently, it was demonstrated that PANI/Te nano-composite could be the future EMI shielding materials for blocking of electromagnetic waves/radiations in X-band. It was hypothesized that the composite which initially has low conductivity can be converted to reasonably higher conducting material by doping with silver and excess Te. The authors showed EMI shielding efficiency of about -10 dB albeit not without the presence of in-situ generated TeO<sub>2</sub>.<sup>36</sup> Exploration of PANI/Te nanocomposites for applications beyond thermoelectricity, such as energy storage and photoconduction, holds significant potential, paving the way for multifunctional and versatile conducting polymer-based materials for diverse energy applications. Furthermore, the development of ternary PANI/SWNT/Te and PANI/MWCNTs-Te nanocomposites demonstrated the feasibility of incorporating multiple components to tailor properties, highlighting avenues for designing high-performance organic-inorganic hybrid materials with enhanced functionality and versatility (figure 5).

**3. PANI-Metal Chalcogenide Nanocomposites:** The research on polymer-based thermoelectric composites, particularly focusing on polyaniline (PANI) and inorganic nanoparticles such as ZnSe, CdSe, CdTe, PbTe, Bi<sub>2</sub>Se<sub>3</sub>, Bi<sub>2</sub>Te<sub>3</sub>, Ag<sub>2</sub>Se, and Bi<sub>0.5</sub>Sb<sub>1.5</sub>Te<sub>3</sub>, as well as mixed metal chalcogenides provide valuable conceptual insights into enhancing thermoelectric performance through tailored nano-structuring and interface engineering. By incorporating these nanoparticles into PANI matrices through diverse synthesis methods,



**Figure 5.** Charge transport mechanism in Te-PANI [Reproduced from ref. 34, with permission from Springer Nature, copyright 2023]

such as solvothermal, electrodeposition and chemical oxidation, researchers have achieved significant improvements in electrical conductivity, Seebeck coefficient and power factor. Utilization of low-dimensional nanostructures and introduction of hybrid interfaces in PANI-based composites have demonstrated promising results in enhancing thermoelectric properties, paving way for potential applications in flexible thermoelectric devices and low-temperature thermoelectric systems. Future research in this domain could focus on further optimizing nano-structuring process, exploring novel synthesis techniques, and elucidating underlying mechanisms governing enhanced thermoelectric performance. Additionally, investigating scalability, long-term stability, and environmental consequence of PANI-based thermoelectric composites would be crucial for their practical implementation in energy harvesting and waste heat recovery applications. This section presents a summarized view of research on PANI-chalcogenide nanocomposites. Polyaniline-chalcogenide nanocomposites are also reported as potential electronic materials.<sup>36-45</sup> Researchers adopted a variety of methods for their synthesis and fabrication of films of the composites and the same are described in Table 2. Selected metal selenides and tellurides are discussed in subsequent sections.

**3.1. PANI/Zinc Chalcogenides:** While having done extensive literature search, we could not retrieve any literature on ZnTe/PANI composites, however there are a few reports emphasizing ZnTe incorporation with other polymers. In view of such lacking information only ZnSe/PANI is being discussed here. This however implies that the researchers may like to indulge in these materials and conduct extensive research to expand utility of ZnTe for electronics and photonics applications. Bormashenko *et al.*<sup>46</sup> conducted research on utilizing films of ZnSe and polyaniline emeraldine base (PANI EB) as coatings to reduce reflection in near and mid-infrared (NIR & MIR) optical region (Figure 6). The PANI coating effectively minimized Fresnel losses at middle and near IR region i.e., between 1.0-6.25 μm wavelength. The investigation also assessed damage threshold of coating under laser irradiation at 1.5 μm of wavelength, indicating that the ZnSe has satisfactory microhardness when coated. Thus, thin PANI EB layers are well-suited for coating infrared (IR) optics elements due to their broad IR transparency, high IR radiation stability under, high optical tolerance, and good surface hardness. These properties make them ideal for various IR optics applications, including antireflective coatings for IR windows and lenses.

Kaushik *et al.*<sup>47(a)</sup> presented findings regarding the creation of diffused polyaniline (PANI)/ZnSe QDs structures through electrochemical method, with potential applications in LEDs. polyaniline films form ordered bundles of closely packed polymeric strands, allowing uniform dispersion of ZnSe QDs. Resulting PANI/ZnSe films exhibit significantly improved luminescence.



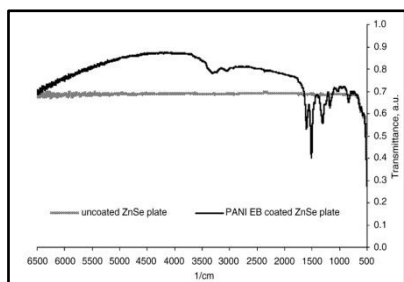


**Figure 6.** Comparison of coated and uncoated ZnSe plates [Reproduced from ref. 46, with permission from Elsevier, copyright 2004]

**Table 2:** Some Polyaniline/Metal Chalcogenide nanocomposites

Material	Synthesis Process	Significant Properties	Ref
CdSe/PANI	Aniline and CdSe NPs were mixed by ultrasonication, then polymerized by APS.	Electronic: conductivity, current density	5
C <sub>60</sub> /CdSe/PANI	C <sub>60</sub> /CdSe was used as promoting agent for polymerization of Aniline.	Optoelectronic & Thermoelectric	37
PANI/CdSe (TPs)	PANI film was dipped in CdSe solution for few seconds.	Optical: PL	38
Cu <sub>2</sub> Se/PANI	In aniline, HCl solution Cu <sub>2</sub> Se NPs were mixed and polymerized by APS.	Optical and electronic	39
PANI-Ag <sub>2</sub> Se/PVDF	PANI layer were coated over Ag <sub>2</sub> Se using dodecylbenzene sulphonic acid.	Thermoelectric	40
PANI-Bi <sub>2</sub> Se <sub>3</sub>	template-based in situ oxidative chemical polymerization by APS after mixing 30% Bi <sub>2</sub> Se <sub>3</sub> NPs in aniline solution.	Thermoelectric	41
PANI- Bi <sub>2</sub> Te <sub>3</sub>	Bi <sub>2</sub> Te <sub>3</sub> nanorod in aniline-SSA solution, then APS added for polymerization.	Thermoelectric	42
Bi <sub>2</sub> S <sub>3</sub> /PANI and Bi <sub>2</sub> Te <sub>3</sub> /PANI	Chalcogenides were sonicated in toluene. Then PANI was added and heated with intermittent sonication.	Thermoelectric	43
PbTe-PANI core-shell	In situ fabrication by dissolving APS in PbTe precursor solution and mixing in aniline-CCl <sub>4</sub> solution for interfacial polymerization.	Thermoelectric	44
PANI/Cu <sub>2</sub> ZnSn Se <sub>4</sub>	PANI was electrodeposited on fluorine doped tin oxide (FTO)/glass electrode. Then CZTSe was electrodeposited on it using aqueous electrolyte solution of its precursors in tartaric acid solution.	Electronic: current density, photocurrent	45
CdTe/PANI	Galvanostatic electrodeposition of PANI on ITO and CdTe doping by soaking solution.	Optoelectronic: Electroluminescence (EL)	46
CdSeTe @ PANI	In CdSeTe QD HCl and aniline were added which was polymerized by adding K <sub>2</sub> S <sub>2</sub> O <sub>8</sub> .	bioimaging	47 (a)

The particle size of ZnSe QDs is 5 nm, which is smaller than the Bohr exciton radius for ZnSe (9 nm).<sup>47(b)</sup> This small size leads to a high density of surface states that trap photoexcited carriers, thereby suppressing excitonic luminescence. However, when PANI is used as a host, it passivates these surface states, enhancing the luminescence of the composite material.

Shirmardi *et al.*<sup>48</sup> investigated the impact of incorporating polyaniline (PANI) on photocatalytic efficacy of ZnSe NPs as organic semiconductor. Co-precipitation method was used to synthesize pristine ZnSe NPs and core-shell ZnSe/PANI type-II heterojunction nanocomposites, thus separating the photogenerated electron-hole pair, reducing its recombination and preparing it for photocatalytic application. The composite showed reduced band-gap value when compared with pristine ZnSe NPs induced by PANI, with shift in VB and CB edges. Photocatalytic assessments for methylene blue (MB) as well as chromate ion removal by the action of visible-light, showed enhanced behaviour of ZnSe/PANI nanocomposites than pure ZnSe NPs due to type-II heterojunction. Outcome from application of Brunauer-Emmett-Teller (BET) theory had highlighted a decrease in nanocomposite textural properties due to PANI, such as specific surface area, pore size and pore volume.

Shokr *et al.*<sup>49</sup> conducted study on synthesis of nanocomposites comprising polyaniline and ZnSe wherein ZnSe nanoparticles, approximately 8.5 nm in size, were produced via colloidal technique, while polyaniline was synthesized alongside the ZnSe nanostructure. XRD analysis revealed semicrystalline nature of polyaniline and cubic crystal structure of ZnSe. SEM images illustrated enlargement in particle size due to integration of ZnSe into the polyaniline matrix. UV-Visible spectroscopy was employed to examine optical characteristics, revealing reduction in energy gap of polyaniline by about 0.5 eV with increased Zn content. Overall  $E_g$  was enhanced from 3.42 to 2.92 eV. ZnSe, being a semiconductor with a wide bandgap, introduces additional electronic states with lowered activation energy within the band structure of PANI. These states can facilitate the generation of more holes due to increased dc conductivity. Specifically, the interaction between the PANI matrix and ZnSe quantum dots can lead to hopping of charge carriers, where electrons from the PANI can be transferred to ZnSe, leaving behind holes in the PANI. This charge transfer process effectively increases the hole concentration in the polyaniline. Thermoelectric power measurements suggested that holes were the predominant carriers, exhibiting increased mobility and quantity, alongside diminished potential barrier with higher ZnSe concentrations within the polyaniline matrix. Jijana *et al.*<sup>50</sup> produced electrochemically polymerized ZnSe quantum dots/PANI nanofibers composites having 3-mercaptopropionic acid-capping on ZnSe. It was reported that the quantum dots are attached with PANI through the carboxylic acid functionality, thus maintaining functionalities from both PANI and QDs surface useful for horseradish peroxidase (HRP) enzyme, a bio-receptor attachment. The biosensor constructed from such composite showed excellent capacity to detect 17 $\beta$ -estradiol under different conditions. The explored research on polyaniline (PANI) and zinc selenide (ZnSe) nanocomposites provides valuable conceptual insights into their multifaceted applications.

The utilization of PANI as antireflection coating for infrared optical elements, in combination with ZnSe, demonstrates its potential to mitigate Fresnel losses and transmit high power density infrared radiation. The creation of PANI/ZnSe through electrochemical methods reveals promising prospects for enhancing luminescence in LED applications and in biosensing. The incorporation of PANI as organic semiconductor in ZnSe nanoparticles significantly improves photocatalytic efficacy, opening avenues for environmental remediation. Additionally, the synthesis of PANI/ZnSe nanocomposites with tailored properties, such as semicrystalline structure and altered optical and electrical characteristics, showcases potential in thermoelectric applications. Looking forward, future scope lies in optimizing synthesis techniques, ensuring scalability, and exploring long-term stability of these nanocomposites. Further research should delve into integration of these materials into practical devices, understanding their performance under diverse conditions, and investigating their environmental impact. Novel combinations of conducting polymers and semiconductors, along with development of multifunctional nanocomposites, could expand horizon of applications in electronics, sensors, and beyond, paving way for technological advancements and real-world implementations.

**3.2. PANI/Cadmium Chalcogenides:** Singh *et al.*<sup>5</sup> had mixed CdSe in aniline and then polymerized it using APS. Three order increase in current density was evaluated as compared to pure PANI. The observed ohmic behaviour in forward bias voltage was attributed to conduction behaviour exhibited by free charge carriers, specifically "polarons and bipolarons".





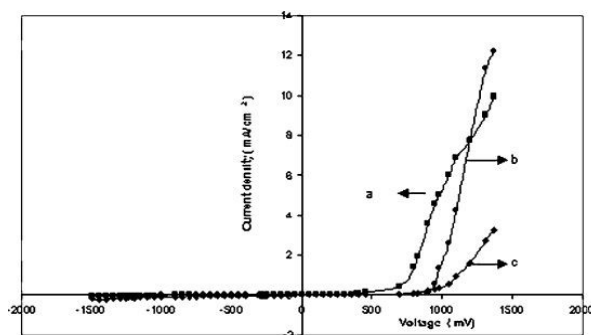


**Figure 7.** Current density v/s Voltage (a) CdS/polyaniline, (b) CdSe/polyaniline, and (c) CdTe/polyaniline [Reproduced from ref. 35, with permission from Springer, copyright 2007]

Prominent presence of cubic phase CdSe had been examined with slightly less lattice constant value of 0.554 nm. Short circuit current density was found to increase to 150 A/cm<sup>2</sup>. Thus, an increase in conductivity of the nanocomposite suits its applications in p-n junction diodes, sensing devices etc. Joshi *et al.*<sup>35</sup> reported the fabrication of heterojunctions by implication of electro-chemically deposited PANI and CdX (X=S, Se, Te) thin films. Ideality factors and flat band potentials were determined for CdS, CdSe, and CdTe-based junctions, indicating their suitability for optoelectronic applications. Heterojunction and diode properties e.g. current and capacitance voltage i.e. I-V and C-V were studied.

Figure 7 (a-c) displays the I-V characteristics of the junction between cadmium chalcogenide and polyaniline. It was shown that CdX/polyaniline may function as diode materials. Not only tellurium based II-VI semiconductors but selenium based can similarly play vital role in development of such composites for photovoltaics. Ahilfi *et al.*<sup>51</sup> synthesized PANI based nanocomposites involving CdSe nanoparticles through chemical and electrospinning method where crystalline cubic CdSe/PVA nanocomposite served as acceptor, while amorphous PANI-DBSA/PS nanofibers acted as donor in hybrid solar cell. Also, the fine dispersion of PANI within the PS film can generate photogenerated electrons and holes when exposed to UV light resulting in increased absorption in near UV range. Patullo *et al.*<sup>52</sup> attempted to enhance the photovoltaic conversion efficiency by utilization of highly conductive materials such as PANI and (PEDOT:PSS) by employing dip-coating technique on pulsed layer deposited CdS/CdTe film as substrate.

The studied show that electrochemically synthesized PANI/CdTe composite on ITO exhibited superior anticorrosion properties than pure polyaniline coatings on stainless steel (XC 70) due to higher tendency of attracting electrons of protonated polyaniline as revealed by electrochemical impedance spectroscopic techniques.<sup>53</sup>

Incorporating fullerene with PANI also attracted the researchers and a study was undertaken by Rusen *et al.*<sup>37</sup> who introduced a new technique to oxidatively polymerize aniline (PANI). They developed a method that employed fullerene C<sub>60</sub>/CdSe QDs to enhance polymerization process. The study also proposed a mechanism for the polymerization process, involving donor-acceptor exchanges between the components based on their HOMO-LUMO energy levels as shown in figure 8. It was an interesting study where size dependent polymerization was discussed showing increased polymerization efficiency with decreasing CdSe particle size. CdSe tetrapods synthesized by solvothermal method were incorporated in PANI film via low-cost chemical bath deposition method by Bhand *et al.*<sup>38</sup> to create void-free, densely packed, granular hybrid PANI/CdSe nanocomposite layers.

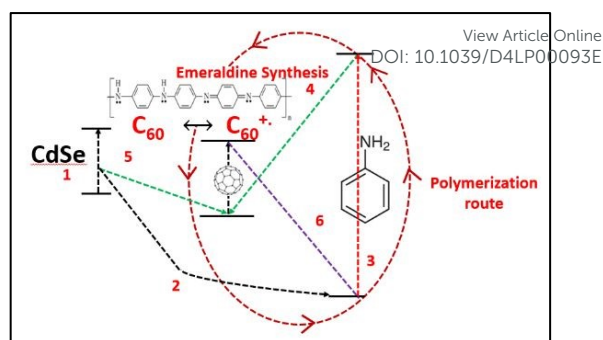


**Figure 8.** Oxidative polymerization of aniline using CdSe-C<sub>60</sub> system [Reproduced from ref. 37, with permission from Nature, copyright 2016]

Enhanced absorption and photoluminescence (PL) intensities were observed in visible to near-infrared (NIR) spectrum by increased dipping time. This augmentation can be attributed to interaction between CdSe and protonated N-H group of PANI. It was shown that thermal stability can be enhanced by presence of CdSe in nanocomposite as compared to pure PANI. In another method, Gaponik *et al.*<sup>54</sup> applied galvanostatic electrodeposition to deposit polyaniline/CdTe nanocomposites on ITO/glass substrate by use of colloidal CdTe and compared the photoluminescence and electroluminescence spectrum to observe a peak at same wavelength of 500 nm (Fig. 9) for the size dependent colour tunability from green to red. Rise of current was examined at lower voltage in CdTe/PANI than CdTe. It was discussed that because of better hole transporting property of polyaniline, CdTe/PANI layer composites showed better Electroluminescence (EL) quantum efficiency. Xue *et al.*<sup>55</sup> observed 40 times enhanced fluorescence by polymerizing aniline on the surface of CdSeTe quantum dots. It had given high amplified signal for cell imaging as fluorescence intensity was increased thousand times with emission wavelength 450 nm when incident with 360 nm light. They observed that if CdSeTe QDs are capped by PANI then surface traps were passivated and absorption and emission bands get blue-shifted. Absorption band shifted from 360 nm to 300 nm and emission band shifted to 450 nm from 560 nm. Characteristic IR band of CdSeTe quantum dot were assigned at 1307 cm<sup>-1</sup> and 1275 cm<sup>-1</sup>. Interaction of amine and carboxylic groups with PANI and quantum dots caused shift in the characteristic peaks of PANI. This study had also shown that CdSeTe/PANI composite was more negatively charged as zeta potential value of CdSeTe & CdSeTe/PANI QDs found to be -29.9 mV & -53.1 mV respectively.

Joshi *et al.*<sup>56</sup> presented LPG sensor with room temperature (300 K), formed by n-CdSe/p-polyaniline junction through electro-chemical deposition method. The forward biased current-voltage characteristics displayed significant shift for dissimilarity in LPG concentrations. The peak response, reaching up to 70%, had been attained with concentration value 0.08 vol% LPG. Similarly, in another research they investigated the response of electrodeposited n-type CdTe and p-type polyaniline heterojunction for sensing liquefied petroleum gas at elevated temperature with notable response characteristics at fixed voltage of +1.38 V for response time ranging from 80 to 300 s, and recovery time of about 600 s depending on the gas concentration.<sup>57</sup> Hybrid polyaniline (PANI) thin layers with CdTe, CdSe, as well as combination of both NPs were fabricated by Verma *et al.*<sup>58</sup> using the spin-coating technique where chemical oxidation method was used for preparation of PANI, while solvothermal method was employed for synthesis of CdTe and CdSe nanoparticles.



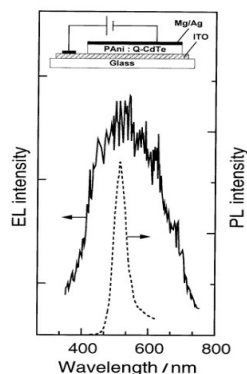


**Figure 9.** PL and EL spectra of CdTe/PANI heterojunction [Reproduced from ref. 54, with permission from Royal Society of Chemistry, copyright 1999]

Absorption spectra revealed formation of charge transfer complexes in hybrid films and the same was studied by cyclic voltammetry. There was another interesting research by Manaf *et al.*<sup>59</sup> who incorporated PANI into glass/FTO/CdS/CdTe/Au diode structures, enhancing photovoltaic activities, particularly open circuit voltage and fill factors. They suggested that PANI, synthesized through electrochemical methods, holds promise being highly efficient and economical, as well as fairly stable inorganic/organic hybrid thin layered solar cells. Also, Junior *et al.*<sup>60</sup> had investigated impact of incorporating polyaniline (PANI) at the junction of CdTe/CdS layers in hybrid solar cells with improved layer contact. The addition of PANI indicated alteration in cell characteristics e.g. the open circuit voltage increased to 0.67 V, current density to 0.3 mA/cm<sup>2</sup>, and overall efficiency improved to 0.15%. Overall, it is realized that binary chalcogenide semiconductors along with conducting polymers can become futuristic and alternate materials for energy application.

Xu *et al.*<sup>61</sup> suggested that presence of oxide can better the electron transport. They developed a two-step in-situ emulsion method to generate TiO<sub>2</sub> nanosheets/CdSe/Polyaniline/Graphene composite for in-situ coating on to stainless steel (304SS) for photocathodic protection, that improves electron transfer and cathodic protection efficiency. According to them, photoelectrochemical performance gets big boost from three things working together viz; broadens absorption range, separating electrons and holes effectively, and having a good conductive network.

Semiconductor/conducting polymer hybrid composites can also be effectively exploited for biomedical sensing applications. An example of such study is made by Liu *et al.*<sup>62</sup> who focused on creating a photoelectrochemical (PEC) aptasensor to identify carbendazim (CBZ), a harmful substance found in pesticide residues, within tomatoes. CdTe-PANI/MoS<sub>2</sub> heterostructure were shown to enhance performance of PEC aptasensor. It was demonstrated by the authors that PEC aptasensor functions on "signal-off" detection mode, where the aptamer (specific nucleic acids) binding to CBZ on the CdTe-PANI@MoS<sub>2</sub> surface hinders electron transfer.

The extensive investigation into polyaniline (PANI) composites with cadmium selenide (CdSe) and cadmium telluride (CdTe) nanoparticles reveals their versatile applications in electronic and optoelectronic devices. These studies demonstrate enhanced electrical conductivity, improved photovoltaic activities, and significant potential for various applications such as p-n junction diodes, gas sensors, and solar cells. The incorporation of CdSe and CdTe nanoparticles not only contributes to increased current density

and conductivity but also influences optical properties, allowing for tunable colour emissions.

DOI: 10.1039/D4LP00093E

Similar to binary semiconductor/PANI hybrids, there is also a good scope for ternary and quaternary semiconductors to combine with conducting polymers and be exploited for a variety of sensing and energy application. In this regard, electrodeposition technique can be employed to synthesize copper zinc tin selenide i.e. CZTSe/PANI.<sup>45</sup> It is further stated that first PANI layer was deposited in potentiostatic mode on FTO/glass substrate followed by electrodeposition of CZTSe to observe an increase in photocurrent to 20 times when compared with CZTSe on FTO/glass alone.

The future scope lies in refining synthesis techniques, optimizing nanocomposite properties, and exploring their integration into scalable devices. Further research avenues include investigating long-term stability, environmental impact, and exploring novel combinations of polymers and different semiconductors for innovative applications in emerging technologies. The potential for tailored nanocomposites with superior performance suggests a promising future for PANI/CdSe/CdTe in diverse electro-, opto- and electronic applications.

**3.3. PANI/Bismuth Chalcogenides:** Polyaniline/Bi<sub>2</sub>Se<sub>3</sub> nanoplates were synthesised using in-situ solvothermal polymerization by Mitra *et al.*<sup>41</sup> where the 2D layered structure showed enhancement in carrier transport properties through hopping model. The power factor of composite was reported to be 30 times as compared to pure PANI with 30% Bi<sub>2</sub>Se<sub>3</sub> content. Subramanian *et al.*<sup>63</sup> investigated the electrodeposition process of thin layers of Bi<sub>2</sub>Se<sub>3</sub> and Bi<sub>2</sub>S<sub>3</sub> films doped with polyaniline (PANI). The optical band gap energy of the initially deposited Bi<sub>2</sub>Se<sub>3</sub> thin film was increased with higher concentrations of PANI. Electrical conductivity assessments revealed Arrhenius behaviour across all films, with PANI dependent activation energies. Reddy *et al.*<sup>43</sup> have reported Bi<sub>2</sub>Te<sub>3</sub> by reacting bismuth oleate and trioctylphosphine telluride (TOP-Te) at about 80°C. To coat polyaniline on it, toluene dispersed polyaniline is refluxed at about 100°C. The so-prepared Bi<sub>2</sub>Te<sub>3</sub> nanorod were coated with PANI to improve the thermoelectric properties. Likewise, Chatterjee *et al.*<sup>64</sup> synthesized PANI/ Bi<sub>2</sub>Te<sub>3</sub> composite employing simultaneous electrochemical and deposition method to obtain rod-like nanostructures of less than 100 nm diameter. UV-Vis. spectra discussed degree of doping in the case of the nanocomposite.<sup>42</sup> The broad band around 634 nm which was originally present in polyaniline disappeared in the nanocomposite spectrum was indicative of organized molecular arrangement along the nanorod axis, sort of diminished  $\pi$ - $\pi^*$  conjugation imperfections within PANI. Likewise, Yadav *et al.*<sup>36</sup> reported UV-Vis of PANI/Te nano-composite in DMF depicting  $\pi$ - $\pi^*$  at 354 and polaron- $\pi^*$  transitions at 382 and 602 nm wavelengths (Fig. 10). The thermoelectric power (S) of PANI/Bi<sub>2</sub>Te<sub>3</sub> composite showed a change due to change in charge carriers from holes to electrons. Core-shell nanocable design having PANI/Bi<sub>2</sub>Te<sub>3</sub> was developed using solvothermal and chemical oxidative process to obtain lower thermal conductivity leading higher thermoelectric power above 380K.<sup>42</sup>

Guo *et al.*<sup>65</sup> explored the enhancement of thermoelectric power in polymer-based composites through carrier energy-filtering action at hybrid organic-inorganic interface. Bi<sub>0.5</sub>Sb<sub>1.5</sub>Te<sub>3</sub> nanoplates (BST NP) were incorporated into camphor-sulfonic acid-doped polyaniline (CSA:PANI) using cryogenic grinding and hot pressing, which formed abundant hybrid interfaces in CSA:PANI/BST NP composites. This configuration increased Seebeck coefficient and power factor substantially, attributing to energy-filtering effect at CSA:PANI/BST NP interface.



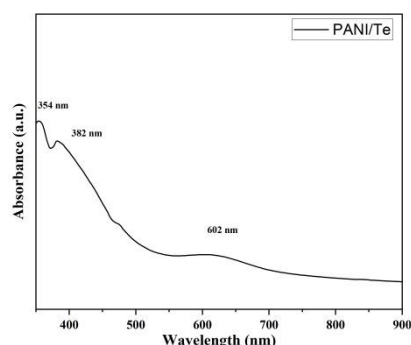


**Figure 10.** UV-Visible spectrum of PANI/Te in DMSO [Reproduced from ref. 36, with permission from Royal Society of Chemistry, copyright 2023]

The resulting  $zT$  values, reaching up to  $8.637 \times 10^{-4}$  at 300 K and  $1.64 \times 10^{-3}$  at 400 K. The enhanced thermoelectric properties demonstrated effectiveness of energy-filtering action in TE materials made from PANI, marking significant advancement in this field. Similarly, Zhmurova *et al.*<sup>66</sup> developed Emeraldine salt type PANI-based nano-thermoelectric materials incorporating  $\text{Te}^0$  and  $\text{Bi}_2\text{Te}_3$  nanoparticles along with multi-walled carbon nanotubes (MWCNT). The research investigated temperature-dependent direct current (DC) electrical conductivity of nanocomposites in 298–353 K. The augmentation of inorganic nanophase content typically boosted the conductivity of ES-PANI/ $\text{Te}^0$  and ES-PANI/ $\text{Bi}_2\text{Te}_3$  nanocomposites.

Hegde *et al.*<sup>67</sup> studied thermoelectric (TE) performance of composites consisting of  $(\text{Bi}_{0.98}\text{In}_{0.02})_2\text{Te}_{2.7}\text{Se}_{0.3}/\text{PANI}$  and  $(\text{Bi}_{0.98}\text{In}_{0.02})_2\text{Se}_{2.7}\text{Te}_{0.3}/\text{PANI}$  in temperature range of 10 to 350 K. The BIS/PANI composite exhibited six-fold decrease in electrical resistivity compared to BIT/PANI sample. The  $zT$  value of BIT/PANI was shown to have increased by 20 times than pure BIT samples, suggesting it to be a potential candidate for low-temperature TE applications. Studies on polyaniline (PANI) composites with bismuth chalcogenides ( $\text{Bi}_2\text{Se}_3$ ,  $\text{Bi}_2\text{Te}_3$ , and  $\text{Bi}_{0.5}\text{Sb}_{1.5}\text{Te}_3$ ) revealed significant improvements in thermoelectrics. For instance, PANI/ $\text{Bi}_2\text{Se}_3$  composites show a 30-fold power factor increase, suggesting future advancements in flexible thermoelectric generators. Doping  $\text{Bi}_2\text{Se}_3$  with PANI enhances optical and electrical properties, making it suitable for high-efficiency optoelectronics. PANI-coated  $\text{Bi}_2\text{Te}_3$  and PANI/Te composites improve thermoelectric performance, with potential applications in waste heat recovery and space technology. Incorporating  $\text{Bi}_{0.5}\text{Sb}_{1.5}\text{Te}_3$  into PANI increases the Seebeck coefficient, useful for microelectronics energy harvesting. These materials also exhibit enhanced conductivity for high-sensitivity sensors and flexible electronics. Future research should optimize synthesis, explore charge dynamics, and integrate these composites into advanced energy storage and environmental monitoring devices.

**3.4. PANI/Silver Chalcogenides:** Park *et al.*<sup>40</sup> synthesised the PANI- $\text{Ag}_2\text{Se}/\text{PVDF}$  composite films through a one-step method, employing electrochemical deposition (figure 11) where nanocomposites were investigated with varying PANI coating cycles to enhance the electrical conductivity with decreasing Seebeck coefficient. The improved power factor with stable performance even after 1000 bending cycles, demonstrated excellent flexibility. When used in a thermoelectric device, the composite generated an output voltage and power at variable temperature range ( $\Delta T$ ), indicating possibility of its application in flexible thermoelectric applications. In another research,  $\text{Ag}_2\text{Te}/\text{PANI}$  nanostructures of core/shell type were successfully synthesized using a one-pot interfacial method.<sup>68</sup>

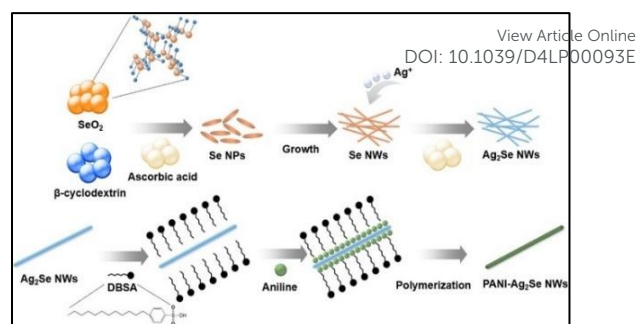


**Figure 11.** Polyaniline- $\text{Ag}_2\text{Se}$  nanowires synthesis [Reproduced from ref. 40, with permission from Elsevier, copyright 2021]

The resulting nanostructures, with sizes ranging from 80 to 100 nm, exhibited a core composed of  $\text{Ag}_2\text{Te}$  nanoparticles of about 10 nm in size. When subjected to cold pressing, the  $\text{Ag}_2\text{Te}/\text{polyaniline}$  composite exhibited enhanced thermoelectric properties compared to pure  $\text{Ag}_2\text{Te}$  and polyaniline powders, with higher Seebeck coefficients and lower thermal conductivity. Core-shell nanocomposite had special microstructure and interface between  $\alpha\text{-Ag}_2\text{Te}$  and PANI gives electrical conductivity ( $4.3 \text{ S/m}$ ) 5 order of magnitudes higher than PANI ( $6.53 \times 10^{-5} \text{ S/m}$ ). The calculated figure of merit ( $zT$ ) value of nanocomposite evaluated to be ( $2.09 \times 10^{-4}$ ) which was a little higher than  $\alpha\text{-Ag}_2\text{Te}$  value of ( $2.00 \times 10^{-4}$ ).

Room temperature thermoelectric studies have been reported for ternary hybrids comprising of PANI, MWCNTs, and binary inorganic selenide nanoparticles.<sup>69</sup> XRD confirmed phase purity, and FTIR indicated strong  $\pi\text{-}\pi$  interactions among PANI and MWCNTs. Electrical behaviour of nanocomposites had been examined, with  $\text{Ag}_2\text{Se}$  NPs/MWCNT/PANI showing p-type characteristics ( $zT$  of 0.012), while  $\text{CuSe}$  NPs/MWCNT/PANI showing excellent n-type thermoelectric behaviour. The study proposed future enhancements using conductive fillers and explores the potential impact of light on thermoelectric efficiency due to the materials' photovoltaic effect. In this type of composite field, the synthesis of  $\text{Ag}_2\text{Te}/\text{PANI}$  core/shell and ternary hybrids MWCNTs, and binary selenides indicated potential of nanocomposites for enhanced thermoelectric properties. Future research could focus on further optimizing synthesis techniques, exploring novel combinations of conductive fillers, and investigating synergistic effects of light on thermoelectric performance, particularly regarding photovoltaic capabilities of materials. This avenue of exploration holds promise for advancing thermoelectric technology and its applications in energy harvesting and conversion.

**3.5. PANI/ Lead Chalcogenides:** Wang *et al.*<sup>44</sup> synthesised  $\text{PbTe}/\text{PANI}$  nanocomposite by interfacial polymerization at room temperature. Core-Shell  $\text{PbTe}-\text{PANI}$ ,  $\text{PbTe}$  nanoparticles and  $\text{PbTe}-\text{PANI}-\text{PbTe}$  three-layer spherical structure were obtained in the nanocomposite. High Seebeck coefficient was observed as compared to its bulk counterpart due to smaller particles size. Decrease in Seebeck coefficient from  $626$  to  $578 \mu\text{VK}^{-1}$  and increase in electrical conductivity from  $1.9$  to  $2.2 \text{ Sm}^{-1}$  was reported in cold press composite pellet between 293 to 373 K. Yet Seebeck coefficient value in composite was highest among PANI,  $\text{PbTe}$  and  $\text{PbTe}$ . Although, Power factor of composite was less than  $\text{PbTe}$  nanoparticles, the extremely low value of thermal conductivity of polymer makes the  $zT$  value of composite higher.



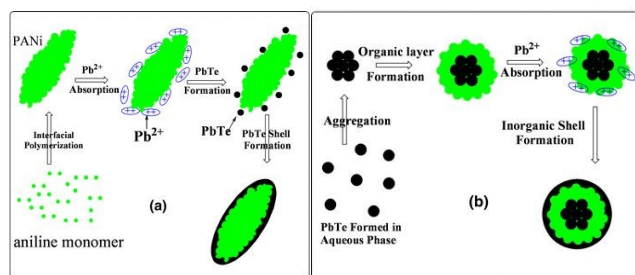


**Figure 12.** Illustration of the growth mechanism for (a) PANI/PbTe core-shell structure and (b) PbTe/PANI/PbTe three-layer nanostructure [Reproduced from ref. 44, with permission from Springer, copyright 2011]

PANI/PbTe core-shell formation mechanism involved PbTe aq. phase and PANI was present at the interface between the aq. phase and carbon tetrachloride ( $\text{CCl}_4$ ) (Water on oil type). It was discussed that the formation of PANI was faster than PbTe. It was hypothesized that initial PANI molecules penetrated to the aqueous phase to absorb  $\text{Pb}^{2+}$  ions, through binding with imino groups of PANI. Such a reaction thus may generate a PbTe shell on PANI core thus finally yielding PbTe/PANI/PbTe nano-composites layers as illustrated in Fig. 12. The process of fabrication of PbTe/PANI nanocomposites had promising prospects for enhancing thermoelectric properties. Future research could optimize synthesis parameters to enhance thermoelectric performance and explore diverse composite systems for broader applications.

**3.6. PANI/Copper Chalcogenides:** On incorporating Copper Selenide ( $\text{Cu}_2\text{Se}$ ) into PANI, Sangamesha *et al.*<sup>39</sup> observed red-shift in UV-Visible absorption band suggesting expanded coil like polymer composite chain. It was also described that due to ordered regularity and aligned nanostructure, shifting and sharpening of quinoid, benzenoid and N-H stretching vibrations are observed in the FTIR spectra. XRD spectra of composite shows the semicrystalline nature of composite having increased PANI/ $\text{Cu}_2\text{Se}$  when compared with pure  $\text{Cu}_2\text{Se}$ . In continuation for betterment of copper selenide either alone or in combination of other metal selenides, Kim *et al.*<sup>70</sup> created two types of nanowire materials,  $\text{Sb}_2\text{Se}_3$  and  $\beta\text{-Cu}_2\text{Se}$ . They synthesized  $\text{Sb}_2\text{Se}_3$  through a hydrothermal reaction and produced  $\beta\text{-Cu}_2\text{Se}$  using a method involving the self-assembly induced by water evaporation. Electrical conductivities of these nanowires were enhanced by forming conducting polymer, PANI, on their surfaces. Various combinations of  $\text{Sb}_2\text{Se}_3$  and  $\beta\text{-Cu}_2\text{Se}$  were used and film made of 70:30  $\text{Sb}_2\text{Se}_3$ :  $\beta\text{-Cu}_2\text{Se}$  with PANI showed value of  $181.61 \mu\text{W}/\text{m}^2\text{K}^2$  as maximum power factor at 473 K. Additionally, a thermoelectric generator (TEG) was assembled using five sections of this film, to realize output power of 80.1 nW with temperature

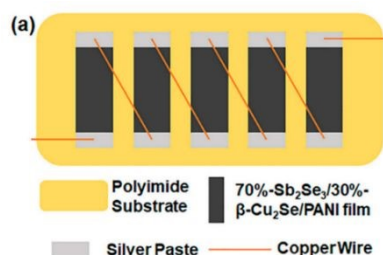


**Figure 13.** TEG structure [Reproduced from ref. 70, with permission from MDPI, copyright 2021]

difference ( $\Delta T$ ) of 30 K (Fig. 13). This research demonstrated potential of flexible TEGs having superior performance with flexibility of polymers, for future power generation in wearable or portable devices. A study conducted by Saray *et al.*<sup>71</sup> explored how combining PANI with  $\text{Cu}_x\text{Se}_y$  improves the photocatalytic performance and several factors were found to be responsible for enhanced activity. The most important one to say was increased porosity of  $\text{Cu}_x\text{Se}_y$ /PANI heterostructure which enhanced absorption of radiation, taking it to higher creation of electron-hole pairs (EHPs). Increased electrical conductivity also facilitated easy transfer of carriers to redox process under light radiation. Additionally, absorption of more photons was responsible for better activities due to presence of PANI. Overall, type-II heterostructure nature of the composite enhanced photocatalytic performance. Photocatalytic experiments targeting dye pollutant degradation in visible light revealed, Ag-PANI exhibited stronger combined effect than pristine PANI composites in rising  $\text{Cu}_x\text{Se}_y$  nanostructure photocatalytic function.<sup>72</sup> The improvement had been ascribed to enhanced textural properties, greater charge transfer, and unique surface plasmon resonance (SPR) properties of Ag NPs, generating photogenerated electrons with higher potential.

**3.7. PANI/Cobalt Chalcogenide:** Sowbakkiyavathi *et al.*<sup>73</sup> synthesized CoSe nanoparticles (NPs) through hydrothermal process, while polyaniline nanofibers (PANI NFs) had been created via chemical polymerization. Subsequently, CoSe/PANI NFs composite formed through ultrasonication. Such a composite was studied for its role as a counter electrode (CE) in dye-sensitized solar cells (DSSC). The CoSe/PANI-based CE demonstrated excellent electrocatalytic action, exhibiting small charge transfer resistance during redox process. Therefore, a higher photocurrent density was achieved for CoSe/PANI nanocomposite (Fig. 14). Notably, the DSSC incorporating the CoSe/PANI CE displayed 9.14% photoconversion efficiency in dark conditions. Gopalakrishnan *et al.*<sup>74</sup> had successfully developed novel binder-free 3D crumpled electrode, composed of  $\text{CoSe}_2$  nanoparticles enveloped in polyaniline (PANI), using co-electrodeposition method on Ni foam ( $\text{PANI}/\text{CoSe}_2/\text{NF}$ ). The three-electrode cell setup showed remarkable results, with specific capacitance of  $1980 \text{ F g}^{-1}$  and specific capacity of  $792 \text{ C g}^{-1}$  at  $2 \text{ A g}^{-1}$ . Also, the electrode exhibited excellent performance in methanol oxidation, demonstrating high current density of  $139 \text{ mA cm}^{-2}$ , low onset potential, and stable current response over 3000 s at 0.5 V. The PANI/ $\text{CoSe}_2$ /NF electrode showed futuristic potential in energy storage, conversion, and catalysis, highlighting its broad impact across various domains. The electrode performed very well when oxidizing methanol, showing consistent current response for 3000 seconds at 0.5V demonstrating its effectiveness.<sup>75</sup>

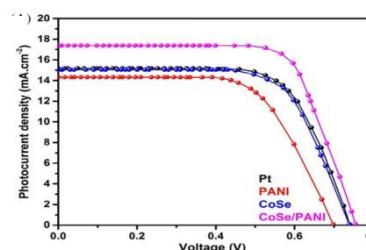


**Figure 14.** DSSC photocurrent density vs voltage (J-V) curve [Reproduced from ref. 73, with permission from Wiley, copyright 2021]



**3.8. PANI/Tungsten Chalcogenides:** Stable and light-sensitive PANI/WSe<sub>2</sub> nanohybrids were reported by Kannichankandy *et al.*<sup>76</sup> as superior catalysts for hydrogen evolution reaction (HER). Showing fast reaction with low overpotential of -190 mV at -10 mA/cm<sup>2</sup>. The infusion of electrons generated by light enhanced production of hydrogen, facilitating utilization of renewable energy sources. This improvement in electrocatalysis was due to reduction in charge transfer resistance achieved through optimizing composition of the nanocomposite. Overall, they achieved notable photoresponsivity and the electrocatalytic hydrogen evolution reaction sustained for about 42 hours. The subsequent mechanism of HER has been depicted in figure 15. In a separate study, Cogal *et al.*<sup>77</sup> synthesized Co-WSe<sub>2</sub>/PANI electrocatalyst via hydrothermal method, having nanosheet structure. PANI played crucial role in augmenting electrochemical surface area and accelerating reaction kinetics and material demonstrated praise worthy electrocatalytic performance in both HER and Oxygen Evolution Reaction (OER). That showed their potential as promising bifunctional electrocatalysts for comprehensive water splitting. Another study where, Sheela *et al.*<sup>78</sup> synthesized polyaniline nanofibers (PANI NFs) through chemical oxidative polymerization procedure and tungsten di-selenide (WSe<sub>2</sub>) NPs via simple hydrothermal method. Electrochemical studies revealed that WSe<sub>2</sub>/PANI (1:1 wt%) CE displayed superior electrocatalytic characteristics for iodide/triiodide reduction compared to other compositions, pristine PANI, WSe<sub>2</sub>, and standard Platinum. Progressive research has unveiled the potential of PANI/WSe<sub>2</sub> nanohybrids and Co-WSe<sub>2</sub>/PANI electrocatalysts in advancing renewable energy technologies. These materials demonstrate remarkable efficiency in hydrogen evolution and water splitting, due to their optimized compositions which enable rapid reaction kinetics and low overpotential. Moreover, WSe<sub>2</sub>/PANI composite nanofibers exhibit superior electrocatalytic behaviour, positioning them as promising alternatives to traditional Pt electrodes in dye-sensitized solar cells. The findings underscore the crucial role of efficient electrocatalysts in driving the transition towards sustainable energy solutions. Future endeavours should focus on refining compositions and scaling up production for widespread deployment in renewable energy systems.

**3.9. PANI/Molybdenum Chalcogenides:** Cogal *et al.*<sup>79</sup> successfully synthesized transition metal-doped MoSe<sub>2</sub>/PANI by catalysing the polymerization of aniline into hydrothermal environment. Structural and morphological analyses revealed formation of flower-like nanoclusters with thin nanosheets, influenced by both transition metal doping (Co, Ni, Fe) and integration of polyaniline (PANI).

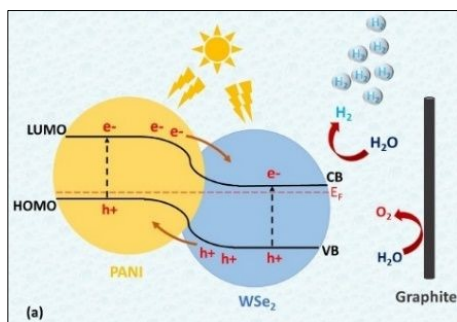


**Figure 15.** Energy band structure with HER and OER in PANI/WSe<sub>2</sub> nanohybrids [Reproduced from ref. 76, with permission from Elsevier, copyright 2021]

Optimal conducting polymer composition was determined to be 100 mg of PANI, and Co-doped MoSe<sub>2</sub>/PANI catalyst demonstrated better performance in both HER and OER in alkaline medium, surpassing Ni- and Fe-doped counterparts. PANI played a crucial role in acting as conducting template for holding transition metal dichalcogenide (TMD) nanosheets and interacting with transition metal, enhancing catalytic activity. Notably, catalyst exhibited high stability for both HER and OER, providing valuable insights for construction of bifunctional electrocatalysts involving TMD materials, conducting polymers, and transition metal doping. Zhang *et al.*<sup>80</sup> found exceptional specific capacitance of MoSe<sub>2</sub>/PANI composite nanospheres, formed by growing layered polyaniline (PANI) on mesoporous MoSe<sub>2</sub> nano-spheres, resulted from synergic interplay between rapid electron mobility of mesoporous MoSe<sub>2</sub> nanospheres and high pseudo-capacitance properties of PANI. The composite electrode exhibited notable specific capacitance of 753.2 Fg<sup>-1</sup> at 1 Ag<sup>-1</sup>, with impressive retention rate of 83% after 15000 cycles. Furthermore, the MoSe<sub>2</sub>/PANI//AC asymmetric supercapacitor (ASC) demonstrated significant energy density of 20.1 Wh kg<sup>-1</sup> having power density of 650 W kg<sup>-1</sup>, providing high-performance supercapacitor electrode materials for advanced application. Mittal *et al.*<sup>81</sup> conducted study to examine how dynamics of charge carriers at interface can be affected in the nanocomposites of MoSe<sub>2</sub>-PANI having different %weight ratios. They experimented such composites for photocatalytic degradation of Rhodamine-B dye and established that 2:1 weight percent ratio of MoSe<sub>2</sub> and PANI promoted better transfer of electrons from PANI to MoSe<sub>2</sub>. This, in turn, reduced recombination rate and improved separation of charges. Consequently, there was a notable enhancement in the efficiency of photocatalytic degradation. Jin *et al.*<sup>82</sup> investigated Goos-Hänchen (GH) shift in Kretschmann configuration when combined with 2D nanomaterials based on surface plasmon resonance (SPR). Theoretical analysis reveals that transition metal dichalcogenides (TMDCs), particularly monolayer MoSe<sub>2</sub>, can enhance GH shift and sensitivity. Varying layers of TMDCs in Ag-TMDCs-PANI/chitosan hybrid structure resulted in both positive and negative GH shifts. The introduction of Cu<sup>2+</sup> ions at concentrations of 30.8530 μM or 2.877 μM significantly altered GH shift, and Ag-WSe<sub>2</sub>-PANI/chitosan structure demonstrated an optimal sensitivity of 2.426 × 10<sup>6</sup> λ/RIU. This suggested potential application of proposed structure in high-sensitivity sensors for chemical, biomedical, and optical sensing.

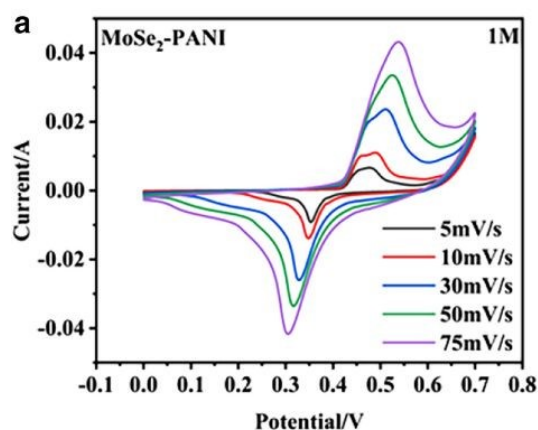


**Figure 16.** CV curves at different scanning rates [Reproduced from ref. 83, with permission from Springer, copyright 2023]



Zheng *et al.*<sup>83</sup> synthesized core-shell MoSe<sub>2</sub>-PANI composite through hydrothermal synthesis. The hollow microspheres demonstrated enhanced active surface area, leading to increased charge storage. The contribution of surface capacitance increment can be estimated by CV curve which showed that contribution was 49% at 5 mV s<sup>-1</sup> and increased to 78% at 75 mV s<sup>-1</sup> (Fig. 16). The MoSe<sub>2</sub>-PANI electrode, having mass ratio of 1:1, displayed highest specific capacitance of 146.5 F g<sup>-1</sup> in certain conditions. Additionally, composite material demonstrated notable energy density of 22.16 Wh kg<sup>-1</sup> and power density of 198 W kg<sup>-1</sup>. Various factors contributed to enhancement of its electrochemical performance.

Chen *et al.*<sup>84</sup> conducted study where they synthesized a new type of material for NH<sub>3</sub> gas sensors. They created composites by combining molybdenum ditelluride (MoTe<sub>2</sub>) nanosheets with polyaniline (PANI) in presence of HCl using in-situ chemical oxidation polymerization approach. Analysis of composite structure revealed porous mesh microstructure with PANI fibers attached to 2D MoTe<sub>2</sub> sheets. The MoTe<sub>2</sub>/PANI composites showed much stronger response to NH<sub>3</sub> gas compared to pure PANI. In particular, composites containing 8 wt.% MoTe<sub>2</sub> showed 4-fold increase in sensitivity 1000 ppm NH<sub>3</sub> due to increased surface area and formation of potential p-n heterojunctions (Fig. 17).

MoSSe/ polyaniline (PANI) was discussed by Khandare *et al.*<sup>85</sup> using hydrothermal and in-situ oxidation polymerization methods, respectively. The composite exhibited high specific capacitance of 340.6 F g<sup>-1</sup> at 1 A g<sup>-1</sup>, coupled with low charge transfer resistance (R<sub>ct</sub>) of 0.33 Ω. Due to interaction between active transition metal dichalcogenide (TMD) materials, thoughtful design involving redox chemistry, and robust storage capacity impressive 99.3% capacitance retention over extended cycles was achieved. These composites demonstrate enhanced catalytic activity, improved energy storage capabilities, and heightened sensitivity in sensors. Future investigations could focus on optimizing synthesis methods, understanding interfacial charge dynamics, exploring novel applications in catalysis and sensing, and ensuring scalability and environmental sustainability of these materials. Additionally, further research could delve into integration of these composites into practical devices and systems for various technological advancements, making easier way for innovative solutions in energy storage, environmental monitoring, and beyond.

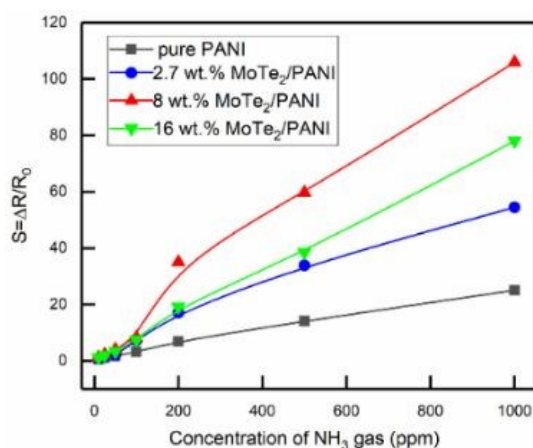


**Figure 17.** Sensing response comparison of composites as a function of NH<sub>3</sub> gas concentration in lab-environment [Reproduced from ref. 84, with permission from MDPI, copyright 2022]

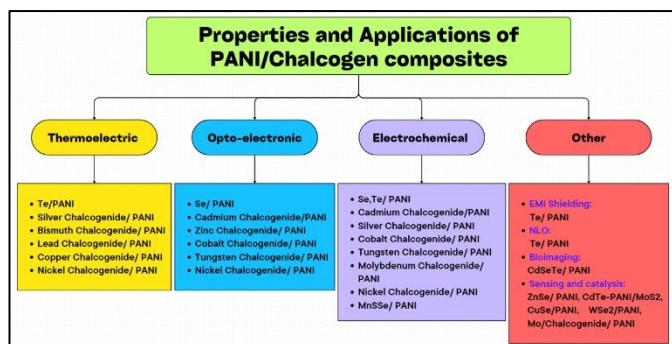
**3.10. PANI/Nickel Chalcogenide & Others:** PANI composite had also been synthesized and studied for other chalcogenides also, e.g. NiSe carbon nanotubes coated with polyaniline composite by Yang *et al.*<sup>86</sup> who generated controlled structure and enhanced electrochemical behaviour. The capacity of 529.3 mAh g<sup>-1</sup> after 100 cycles at 0.1 Ag<sup>-1</sup> was realized when the researchers used NSC/PANI as an anode material. Ion diffusion behaviour analysis revealed stable diffusion rate during cycling. The NSC/PANI//AC LICs exhibited high capacity, retention, and excellent rate performance, that achieved energy density of 53.1 Wh kg<sup>-1</sup> at power density of 1995.41 W kg<sup>-1</sup>. Ju *et al.*<sup>87</sup> employed combination of DBSA/PANI and coated tin selenosulphide i.e., SnSe<sub>0.8</sub>S<sub>0.2</sub> to synthesise PANI-SnSeS nanosheets and utilized in flexible thermoelectric generators. The optimization of thermoelectric performance was dependent on coating cycles. The study introduced solution-based method for incorporating PANI-SnSeS into PVDF matrix, in 2:1 weight ratio to exhibit remarkable durability with much enhanced thermoelectric outcome of about ~134 μW/m·K<sup>2</sup> as a peak power factor at 400 K. Sowbakkivathi *et al.*<sup>88</sup> synthesized NiSe-embedded PANI nanofibers to be used as counter electrodes in dye-sensitized solar cells (DSSCs). This composite material demonstrated superior electrocatalytic activity and achieved higher photo-conversion efficiency compared to pristine NiSe, PANI, and Pt counter electrodes. Aside from this, Yasoda *et al.*<sup>89</sup> produced a MnSSe/PANI heterostructure. They used a one-step solvothermal approach to replace S atoms with Se to generate MnSSe, upon which recrystallization of PANI nanorods was performed, increasing conductivity and electroactive sites. This activity improved the material's crystallinity, allowing charge carriers to move more easily in electrochemical reactions. This resulted in a 1.7 times higher specific capacitance for the MnSSe/PANI heterostructure than for the individual components. The researchers also worked on metal composites containing PANI.<sup>90-93</sup> Oxygen reduction had been accomplished by 4 electron processes in composite consisting of molybdenum-doped ruthenium selenide in polyaniline matrix (PANI+MRS).<sup>94</sup> The material had accessed this property because of good conductivity and electrocatalytic property.

#### 4. Applications

Various polyaniline composites with Se and Te and their metal chalcogenides have found range of applications, e.g. in thermoelectric, optoelectronic, photocatalytic, sensors, Bioimaging and EMI Shielding (Scheme 2). Most of such applications and purposes are discussed in respective section as part of the materials that have been reviewed above. Still a few additional examples are presented in this section to further bring useful information in one place. Since same or similar materials are used for different applications, they have been discussed as and when required.

For thermoelectric applications, mostly polyaniline composites with silver, bismuth, lead, copper, nickel chalcogenides and tellurium have been studied. The power factor (PF) is reported to increase with Te content in the composite. The highest value has been obtained for Te-nanorod/PANI composite having value of 101 μW/m·K<sup>2</sup> that had 70 wt% Te.<sup>28</sup> Te nanorod/PANI with 60 wt% Te has PF of 50 μW/m·K<sup>2</sup>.<sup>32</sup> However, ternary composites like PANI/SWNT/Te nanorod (43:47:10 wt% ratio), showed PF increase upto 100 μW/m·K<sup>2</sup>.<sup>30</sup> While for PANI/MWCNT/Te nanorod with 50 wt% Te, PF remains approx. 50 μW/m·K<sup>2</sup>.<sup>31</sup> The electrodeposited film of Te on phenolic foam coated PANI, shows increase in Seebeck coefficient from 225 μV K<sup>-1</sup> at 300 K to 342 μV K<sup>-1</sup> at 473 K.<sup>25</sup> Te nanorod (70%)/PANI has also shown increase in P.F. with temperature, that has gained 25 μW/m·K<sup>2</sup> with increase of 150 K.<sup>28</sup>





**Scheme 2.** Properties and applications of various Chalcogen, Chalcogenide/ PANI composites

Similarly, for electrochemical applications the composites of polyaniline with large variety of metals such as cadmium, silver, cobalt, tungsten, molybdenum, nickel, manganese chalcogenides and Se, Te have been studied.

The electrochemical and energy storage properties have been possessed by many PANI/Chalcogen composites. The graphene encapsulated Se nanowire/PANI composite possess reversible charge-discharge capacity of 567 mAhg<sup>-1</sup> at 0.2 C, and 510.9 mAhg<sup>-1</sup> at 2C. Se nanowire offers short diffusion length to Li-ion, PANI shell increases electrical conductivity by passivating surface states and also gives structural stability against charging-discharging. While, further encapsulation with graphene nanosheets improves the electrical conductivity by reducing charge transfer resistance, fastening the Li-ion diffusion.<sup>22</sup> In Te<sub>x</sub>S<sub>y</sub>@PANI nanorod materials for Li-Te<sub>x</sub>S<sub>y</sub> battery, at low charging rate (C-rate) of 0.1 A g<sup>-1</sup> it works as Li-S battery having high capacity of 1141 mAhg<sup>-1</sup>, while at high C-rate of 5 A g<sup>-1</sup> it shows Li-Te battery behaviour with excellent cycling ability.<sup>33</sup> Specific capacitance was highest for 10%-Te/PANI. Higher Te content reduces ion migration and improved stability.<sup>34</sup> Te/PANI (5-15%) showed ohmic behaviour in the dark and photo transport with variable resistance under illumination, with 10% Te/ PANI exhibiting the lowest resistance and highest photo current. Te doping enhanced conductivity and photo carrier generation, with 10% Te @ PANI showing superior performance.<sup>34</sup>

NiSe/CNT@PANI nanofibers can be used in Li-ion capacitors (LIC) as anode material. At power density of 199.5 WKg<sup>-1</sup>, energy density was 91.7 W Kg<sup>-1</sup> and at higher power density of 1995.4 WKg<sup>-1</sup>, energy density comes out to be 53.1 WKg<sup>-1</sup>, found in the fabricated LSC.<sup>86</sup> NiSe/PANI nanofibers can be used in DSSC as counter electrode (CE) reaching upto photoconversion efficiency of 8.46%. It showed better electrocatalytic behaviour than pristine PANI and NiSe CE.<sup>88</sup> The applications for other composites have been briefly discussed in the main sections (Scheme 2).

For optoelectronic applications, combination of polyaniline with chalcogenides of cadmium, zinc, cobalt, tungsten, nickel as well as individual elements Se and Te have been documented in the literature. Typically, CdSeTe QDs capped with PANI had gained enhanced fluorescence and blue shift in emission bands due to surface trap passivation by PANI. For cell imaging it is a potentially good material having 1000 times increase in fluorescence at 450 nm when radiated with 360 nm. Zeta potential in the QD has increased from -29.9 mV to -53.1 mV upon PANI capping.

Rare application of such composites in EMI has been reported by us in the recent past. In such a unique study authors incorporated

silver metal to enhance electrical conductivity that eventually yielded useful EMI shielding to the tune of about -10dB. The composite also involved PVA to assist in film fabrication. Te nanowire coated with PANI, having broom shaped hierarchical structure has been found to have non-linear optical (NLO) property.

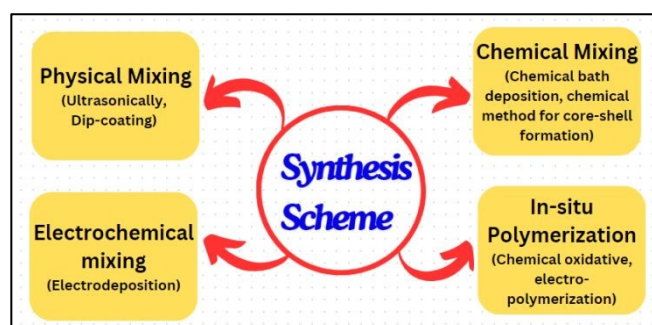
## 5. General Synthesis of Composites of PANI with Chalcogenides

The polymerization of aniline is accomplished by mainly two methods: chemical oxidative polymerization & electrochemical polymerization. And, the chalcogenides can be prepared by using chemical methods such as solvothermal, hydrothermal, colloidal, sol-gel; electrochemical deposition and physical layer deposition (PLD). But to produce composites of PANI with chalcogens and chalcogenides, the synthesis scheme can be majorly categorized into four ways: (i) Physical mixing, (ii) Chemical mixing, (iii) Electrochemical mixing, and (iv) Catalytic in-situ polymerization. Physical mixing can be accomplished by ultrasonic mixing or dip coating or incorporation of nanoparticles into the polymer matrix or spin coating. Some examples of the PANI/ chalcogen composites formed in this way are PANI/Se<sup>20</sup>, Cu<sub>2</sub>Se/PANI<sup>39</sup>, PANI/PEDOT:PSS/CdTe<sup>52</sup>, CSA:PANI/BST<sup>65</sup>, CoSe/PANI<sup>73</sup>.

The chemical mixing is accomplished mainly by co-precipitation. The composite materials produced in this way are core-shell structures (ZnSe/PANI<sup>48</sup>, PANI/Bi<sub>2</sub>Te<sub>3</sub><sup>42</sup>, PbTe/PANI/PbTe<sup>44</sup>, Ag<sub>2</sub>Te/PANI<sup>68</sup>, MoSe<sub>2</sub>/PANI<sup>83</sup>), PANI/SWNT/Te<sup>30</sup>, PANI/Te<sup>32</sup>, ZnSe/PANI<sup>47(a),49</sup>, Co-WSe<sub>2</sub>/PANI.<sup>77</sup> Electrochemical mixing is accomplished by electrochemical deposition of PANI on chalcogenide material forming heterostructure or intermixed composite. Some of these composites following this way are Te/phenolic foam/PANI<sup>25</sup>, PANI/Se-Te<sup>29</sup>, CdX (X=S, Se, Te)/PANI<sup>35</sup>, ZnSe/PANI<sup>50</sup>, CdTe/PANI<sup>54,58</sup>.

For catalytic in-situ polymerization chalcogenides were first formed and dispersed in a solvent and polymerization of aniline is performed in-situ through chemical oxidative polymerization. Here, the polymerization happens due to catalytic action. The good example of this is reported by Yadav et al for Te/PANI nanocomposite.<sup>36</sup> Other such composites formed by this method are Se/PANI<sup>19,21</sup>, SeF/PANI<sup>24</sup>, Te/PANI<sup>27</sup>, CdSe/PANI<sup>5</sup>, C<sub>60</sub>/CdSe/PANI<sup>37</sup>, PANI/Bi<sub>2</sub>Se<sub>3</sub><sup>41</sup>, MoTe<sub>2</sub>/PANI<sup>84</sup>, MoSSe/PANI<sup>85</sup>.

Another version of the in-situ polymerization happens when aniline is electropolymerized in/on chalcogenide. The composites and heterostructures formed this way are PANI/CoSe<sub>2</sub>/Ni foam<sup>74</sup>, CZTSe/PANI (Scheme 3).<sup>45</sup>



**Scheme 3.** Various synthesis methods of PANI/Chalcogen nano-composites

## 6. Conclusions



The present article is a brief yet informative review on Se, Te and their metal chalcogenides (two of the most versatile elements of the chalcogen group). These are studied by large number of researchers in combination with polyaniline to classify them as PANI/chalcogenide nano-composite materials, emphasizing their thermoelectric and electrochemical properties and their potential for energy conversion. Additionally, several researchers reported on the chemical synthesis and characterization of tellurium-doped polyaniline, electrodeposition of tellurium films, and the synthesis of a PANI/Te nanocomposites with improved nonlinear optical properties. These findings offer promising avenues for the development of efficient energy utilization systems and multifunctional materials, addressing the challenges posed by the global energy crisis. The preparation and characterization of PANI with selenium demonstrated significant improvements in electrical conductivity, thermal stability and field emission properties making them as useful materials in various electronic applications, such as vacuum micro-nano-electronic devices. From enhanced thermoelectric properties to improved fluorescence and biocompatibility, these materials hold promise for addressing various scientific and technological challenges. The synthesis methods discussed in various articles covered in this review, pave the way for further advancements in the field of nanocomposite materials. Recent research has extensively explored multifaceted applications of polyaniline (PANI) composites, particularly when combined with various semiconductor nanoparticles such as CdSe, CdTe, and other metal chalcogenides. These studies have provided valuable insights into potential of PANI-based nanocomposites in electronic devices, optoelectronics, and thermoelectric applications. By incorporating semiconductor nanoparticles into PANI matrices through diverse synthesis methods, researchers have achieved significant improvements in conductivity, photovoltaic activities, and sensing capabilities. For instance, successful fabrication of PANI/CdSe and PANI/CdTe nanocomposites has demonstrated enhanced electrical conductivity, improved photovoltaic activities, and potential applications in P-N junction diodes, gas sensors, and solar cells. Furthermore, integration of metal chalcogenides such as MoSe<sub>2</sub> with PANI has shown promise in enhancing thermoelectric performance, paving way for potential applications in flexible thermoelectric devices and low-temperature thermoelectric systems. These advances highlight versatility and promise of PANI-based composites in various technological fields. Looking ahead, future research efforts likely to focus on refining synthesis techniques, optimizing nanocomposite properties, and exploring their integration into scalable devices. Additionally, addressing challenges related to stability, environmental impact, and performance optimization will be crucial for realizing full potential of PANI-based composites in advancing technology and addressing societal needs.

### Author Contributions

Alok Yadav completed literature review, prepared draft of the review article, made some drawings and edited.

Naeem Mohammad cross verified literature and the article along with correctness of the figures and references and obtained all copyright permissions also made some drawings, review and edited draft.

Pawan Khanna reviewed the literature articles and edited the review draft, corrected, improved and finalized the manuscript along with students.

Yogendra Kumar Mishra edited the received article and offered valuable suggestion in term of applications and synthesis methods.

Elham Chamanehpour checked and corrected various sections and edited the manuscript in consultation with Yogendra Kumar Mishra.

### Conflicts of interest

There are no conflicts to declare.

### Acknowledgements

Authors thank Vice-chancellor DIAT for encouragement and support. NM thanks Govt of India for DST INSPIRE fellowship for doctoral research (fellow no. IF200413). YKM acknowledges the fundings from the ESS lighthouse on hard materials in 3D, SOLID (Danish Agency for Science and Higher Education, grant number 8144-00002B), Denmark, TORCH: (Interreg Deutschland-Denmark and the European Union under grant number 04-3.2-23 2, and NANOChem (national infrastructure UFM 5229-00010B, NANOChem, Denmark)

### References

1. H. Shirakawa, E. J. Louis, A. G. MacDiarmid, C. K. Chiang and A. J. Heeger, *J. Chem. Soc., Chem. Commun.*, 1977, 578-580.
2. A. J. Heeger, *J. Phys. Chem. B*, 2001, 105, 8475-8491.
3. Z. Li, Y. Shen, Y. Li, F. Zheng, L. Liu, X. Liu, D. Zou, *High Perform Polym*, 2019, 31, 178-185.
4. A. Eftekhari, L. Li, Y. Yang, *J. Power Sources*, 2017, 347, 86-107.
5. R. Singh, A. K. Shrivastava, A. K. Bajpai, *Mater. Res. Express*, 2019, 6, 1250a9.
6. K. G. B. Alves, E. F. De Melo, C. A. S. Andrade, C. P. De Melo, *J Nanopart Res*, 2013, 15, 1-11.
7. S. Koul, R. Chandra, S.K. Dhawan, *Polymer*, 2000, 41, 9305-9310.
8. M. Khalid, A. M. B. Honorato, H. Varela, "Polyaniline: Synthesis Methods, Doping and Conduction Mechanism", *IntechOpen*, 2018, 1-17. (doi: 10.5772/intechopen.79089.)
9. F. X. Perrin, C. Oueiny, *React Funct Polym*, 2017, 114, 86-103.





## Journal Name

## ARTICLE

10. A. Samadi, M. Xie, J. Li, H. Shon, C. Zheng, and S. Zhao, *Chem Eng J*, 2021, 418, 129425.
11. Shumaila, G. B. V. S. Lakshmi, M. Alam, A. M. Siddiqui, M. Zulfeqar, M. Husain, *Curr. Appl. Phys.*, 2011, 11, 217-222.
12. A. Sezer, U. Gurudas, B. Collins, A. Mckinlay, D. M. Bubb, *Chem Phys Lett*, 2009, 477, 164-168.
13. R. Li, Z. Li, Q. Wu, D. Li, J. Shi, Y. Chen, S. Yu, T. Ding, C. Qiao, *J. Nanoparticle Res.*, 2016, 18, 1-11.
14. L. Zhang, T. Liu, R. Ren, J. Zhang, D. He, C. Zhao, H. Suo, *J Hazard Mater*, 2020, 392, 122342.
15. A. N. Gheymasi, Y. Rajabi, E. N. Zare, *Opt Mater*, 2020, 102, 109835.
16. A. S. Roy, K. R. Anilkumar, M. V. N. A. Prasad, *J Appl Polym Sci*, 2012, 123, 1928-1934.
17. V. V. A. Thampi, S. Thanka Rajan, K. Anupriya, B. Subramanian, *J. Nanoparticle Res.*, 2015, 17, 1-12.
18. R. B. Gapusan, M. D. L. Balela, *Polymer Bulletin*, 2022, 79, 3891-3910.
19. E. Bormashenko, R. Pogreb, S. Sutovski, A. Shulzinger, A. Sheshnev, A. Gladkikh, *Synth Met*, 2003, 139, 321-325.
20. Shumaila, S. Parveen, M. Alam, A. M. Siddiqui, M. Husain, *J Nanosci Nanotechnol*, 2015, 15, 2835-2839.
- 20(a). R. H. Fowler and L. W. Nordheim, *Electron Emission in Intense Electric Fields*, *Proc. The Royal Soci.* (1928), 119, 173-181.
21. E. Ozkazanc, S. Zor, H. Ozkazanc, *J Macromol Sci B*, 2012, 51, 2122-2132.
22. J. Zhang, Y. Xu, L. Fan, Y. Zhu, J. Liang, Y. Qian, *Nano Energy*, 2015, 13, 592-600.
23. W. Ye, K. Wang, W. Yin, W. Chai, Y. Rui, B. Tang, *Dalton Transactions*, 2019, 48, 10191-10198.
24. Z. K. Heiba, M. B. Mohamed, N. G. Imam, *J Supercond Nov Magn*, 2019, 32, 2981-2986.
25. C. H. Jiang, W. Wei, Z. M. Yang, C. Tian, J. S. Zhang, *J. Porous Mater.*, 2012, 19, 819-823. DOI: 10.1039/D4LP00093E
26. S. Kazim, V. Ali, M. Zulfeqar, M. M. Haq, M. Husain, *Curr. Appl. Phys.*, 2007, 7, 68-75.
27. J. Wang, X. Zhang, R. Ke, S. Zhang, C. Mao, H. Niu, J. Song, S. Li, Y. Tian, *Semicond Sci Technol*, 2016, 31, 1-10.
28. Y. Wang, S. M. Zhang, Y. Deng, *J Mater Chem A Mater*, 2016, 4, 3554-3559;
29. T. Xue, X. Wang, S. K. Kwak, J. M. Lee, *Ind Eng Chem Res*, 2013, 52, 5072-5078.
30. L. Wang, Q. Yao, W. Shi, S. Qu, L. Chen, *Mater Chem Front*, 2017, 1, 741-748.
31. Y. Wang, C. Yu, M. Sheng, S. Song, and Y. Deng, *Adv Mater Interfaces*, 2018, 5, 3-8.
32. Y. Wang, C. Yu, G. Liu, M. Sheng, Y. Deng, *Mater Lett*, 2018, 229, 293-296.
33. J. Li, Y. Yuan, H. Jin, H. Lu, A. Liu, D. Yin, J. Wang, J. Lu, S. Wang, *Storage Mater*, 2019, 16, 31-36.
34. P. Rani, Y. Jewariya, K. K. Haldar, R. Biswas, P. S. Alegaonkar, *J Mater Sci Mater Electron*, 2023, 34, (doi: 10.1007/s10854-022-09414-z).
35. S. S. Joshi, C. D. Lokhande, *J Mater Sci*, 2007, 42, 1304-1308.
36. A. K. Yadav, N. Mohammad, P.K. Khanna, *Materials Advances*, 2023, 4, 4409-4416.
37. E. Rusen, A. Diacon, A. Mocanu, and L. C. Nistor, *Sci Rep*, 2016, 32237. (doi: 10.1038/srep32237)
38. G. R. Bhand, M. G. Lakhe, A. B. Rohom, P. U. Londhe, S. K. Kulkarni, N. B. Chaure, *J Mater Sci Mater Electron*, 2017, 28, 12555-12563.
39. M. A. Sangamesha, K. Pushpalatha, G. L. Shekar, *Ind J Adv Chem Sci*, 2014, 2, 223-227.
40. D. Park, M. Kim, J. Kim, *J Alloys Compd*, 2021, 884, 161098.



## REVIEW ARTICLE

## RSC Applied Polymers

41. M. Mitra, C. Kulsi, K. Kargupta, S. Ganguly, D. Banerjee, *J Appl Polym Sci*, 2018, 135, 46887.
42. K. Chatterjee, M. Mitra, K. Kargupta, S. Ganguly, D. Banerjee, *Nanotechnology*, 2013, 24, 215703.
43. V. B. Reddy, P. L. Garrity, K. L. Stokes, *MRS Online Proceedings Library*, 2003, 793, 354-358.
44. Y. Y. Wang, K. F. Cai, J. L. Yin, B. J. An, Y. Du, X. Yao, *J. Nanoparticle Res.*, 2011, 13, 533-539.
45. K. Urazov, M. Dergacheva, A. Tameev, O. Gribkova, K. Mit, *J. Solid State Chem.*, 2021, 25, 237-245.
46. E. Bormashenko, R. Pogreb, S. Sutovski, A. Shulzinger, A. Sheshnev, G. Izakson, A. Katzir, *Synth Met*, 2004, 140, 49-52.
- 47(a). D. Kaushik, M. Sharma, R. Raj Singh, D. K. Gupta, R. K. Pandey, *Mater Lett*, 2006, 60, 2994-2997.
- 47(b). N. Kumbhojkar, S. Mahamuni, V. Leppert, S.H. Risbud, *Nanostruct. Mater.* 10 (2) (1998) 117.
48. A. Shirmardi, M. A. M. Teridi, H. R. Azimi, W. J. Basirun, F. Jamali-Sheini, R. Yousefi, *Appl Surf Sci*, 2018, 462, 730-738.
49. F. S. Shokr, S. A. Al-Gahtany, *Polym Compos*, 2018, 39, 1724-1730.
50. A. N. Jijana, *Appl Biochem Biotechnol*, 2023, 195, 3425-3455.
51. D. N. Ahilfi, A. S. Alkabb, K. A. Mohammed, and K. M. Ziad, *IOP Conf. Series: Materials Science and Engineering*, 2020, 928, 072069.
52. M. Patullo and M. A. Sahiner, "PANI and PEDOT:PSS Dip-Coating on CdS/CdTe Solar Cells," 2018. [Online]. Available: <https://scholarship.shu.edu/locus/vol1/iss1/9>
53. L. Mekhiche, N. Maouche, B. Nessark, L. Toukal, and H. Ayadi, *J Adhes Sci Technol*, 2021, 35, 2602-2624.
54. N. P. Gaponik, D. V. Talapina, A. L. Rogach, *Phys. Chem. Chem. Phys.*, 1999, 1, 1787-1789.
55. J. Xue, X. Chen, S. Liu, F. Zheng, L. He, L. Li, Jun-Jie Zhu, *ACS Appl Mater Interfaces*, 2015, 7, 19126-19133.
56. S. S. Joshi, C. D. Lokhande, S. H. Han, *Sens Actuators B Chem*, 2007, 123, 240-245.
57. S. S. Joshi, T. P. Gujar, V. R. Shinde, C. D. Lokhande, *Sens Actuators B Chem*, 2008, 132, 349-355. DOI: 10.1039/D4LP00093E
58. D. Verma, V. Dutta, *J. Appl. Phys.*, 2009, 105, 034904.
59. N. A. Abdul-Manaf, O. K. Echendu, F. Fauzi, L. Bowen, I. M. Dharmadasa, *J Electron Mater*, 2014, 43, 4003-4010.
60. P. H. F. M. Junior, A. F. L. Almeida, R. L. Moreiraa, E. S. Teixeira, V. F. Nunesa, D. C. Pinhoa, F. N. A. Freire, *Materials Research*, 2021, 24, 1-9.
61. D. Xu, M. Yang, Y. Liu, R. Zhu, X. Lv, C. Zhang, B. Liu, *J Alloys Compd*, 2020, 822, 153685
62. D. Liu, Q. Gong, X. Xu, S. Meng, Y. Li, and T. You, *J. Electroanal. Chem.*, 2023, 930, 117143.
63. S. Subramanian, D. P. Padiyan, *Mater Chem Phys*, 2008, 107, 392-398.
64. K. Chatterjee, A. Suresh, S. Ganguly, K. Kargupta, D. Banerjee, *Mater Charact*, 2009, 60, 1597-1601.
65. C. Guo, F. Chu, P. Chen, J. Zhu, H. Wang, L. Wang, Y. Fan, W. Jiang, *J Mater Sci*, 2018, 53, 6752-6762.
66. A. V. Zhmurova, G. F. Prozorova, M. V. Zvereva, *Powders*, 2023, 2, 540-561.
67. G. S. Hegde, A. N. Prabhu, S. Putran, M. Y. Bhat, and P. D. Babu, *J Mater Sci: Mater Electron* 2023, 34, 1896.
68. Y. Y. Wang, K. F. Cai, J. L. Yin, Y. Du, X. Yao, *Mater Chem Phys*, 2012, 133, 808-812.
69. A. S. Kshirsagar, C. Hiragond, A. Dey, P. V. More, P. K. Khanna, *ACS Appl Energy Mater*, 2019, 2, 2680-2691.
70. M. Kim, D. Park, and J. Kim, *Polymers* 2021, 13, 1518.
71. A. M. Saray, H. Azimi, A. Shirmardi, M. Nouri, R. Yousefi, *J Alloys Compd*, 2023, 951, 169827.
72. A. M. Saray, H. Azimi, A. Shirmardi, M. Nouri, R. Yousefi, *Surfaces and Interfaces*, 2023, 42, 103416.



73. E. S. Sowbakkivavathi, V. Murugadoss, R. Sittaramane, R. Dhanusuraman, S. Angaiah, *Polym Adv Technol*, 2021, 32, 3137-3149.
74. A. Gopalakrishnan, S. Badhulika, *Mater Chem Phys*, 2021, 273, 125118.
75. A. Gopalakrishnan, S. Badhulika, *J Energy Storage*, 2021, 41, 102853.
76. D. Kannichankandy, P. M. Pataniya, C. K. Sumesh, G. K. Solanki, V. M. Pathak, *J Alloys Compd*, 2021, 876, 160179
77. S. Cogal, G. Celik Cogal, M. Mičušík, M. Kotlár, M. Omastová, *Int J Hydrogen Energy*, 2024, 49, 689-700
78. S. E. Sheela, V. Murugadoss, R. Sittaramane, S. Angaiah, *Solar Energy*, 2020, 209, 538-546.
79. S. Cogal, G. C. Cogal, M. Mičušík, A. Michalcova, M. Šlouf, M. Omastová, *J. Electroanal. Chem.*, 2023, 946, 117728.
80. H. Zhang, G. He, D. Zheng, H. H. Fu, Y. Li, Y. Mi, M. Wu, H. Yuan, *Nanotechnology*, 2023, 41, 28-34.
81. H. Mittal, M. Khanuja, *Mater Today Proc*, 2020, 28, 314-316.
82. M. Jin, J. Liu, W. Xu, D. Deng, L. Han, *Plasmonics*, 2023, 18, 1129-1141.
83. D. Zheng, G. He, Y. Mi, H. H. Fu, Y. Li, H. Zhang, M. Wu, H. Yuan, *J. Mater. Sci. Mater. Electron.*, 37, 2023, 1734.
84. X. Chen, X. Chen, X. Ding, X. Yu, *Chemosensors*, 2022, 10, 1-15.
85. L. N. Khandare, D. J. Late, N. B. Chaure, *Surf. Interfaces*, 2023, 43, 103533.
86. F. Yang, Z. Zhang, H. Li, W. Dong, M. Li, M. Zhao, M. Xue, Q. Zhang, *Mater Today Commun*, 2024, 38, 107816.
87. H. Ju, D. Park, J. Kim, *ACS Appl Mater Interfaces*, 2018, 10, 11920-11925.
88. E.S. Sowbakkivavathi, Vignesh Murugadoss, Saradh Prasad Rajendra, Mohamad S AlSalhi, Preethi Dhandapani, Subramania Angaiah, *Journal of Molecular Structure* 1305 (2024) 137735.
89. K. Yamini Yasoda, Mohd Afshan, S. Charis Caroline, F.M. Harini, Kaushik Ghosh, Sudip Kumar Batabyal, *Electrochimica Acta* 480 (2024) 143879.
90. Ahmet Güngör, Süleyman Gokhan Çolak, Melis Ozge Alas, Çolak, Rûkan Genç, Emre Erdem, *Electrochimica Acta* 480 (2024) 143924.
91. K.Y. Yasoda, S. Kumar, M.S. Kumar, K. Ghosh, S.K. Batabyal, *Materials Today Chemistry* 19 (2021) 100394.
92. Mohit Khosya, Dheeraj Kumar, Mohd Faraz, Neeraj Khare, *International Journal of Hydrogen Energy* 48 (2023) 2518-2531.
93. Swapnika Suresh, Hridya C. Prakash, M. Sathish Kumar, Sudip K. Batabyal, *Journal of Science: Advanced Materials and Devices* 8 (2023) 100639.
94. Nicolas Alonso-Vante, Sandro Cattarin, Marco Musiani, *Journal of Electroanalytical Chemistry* 481 (2000) 200-207.

